Density Functional Theory (DFT) Calculations of the Infrared Absorption Spectra of Acetaminophen Complexes Formed with Ethanol and Acetone Species

Y. Danten,* T. Tassaing, and M. Besnard

Laboratoire de Physico-Chimie Moléculaire (U.M.R C.N.R.S 5803), Université Bordeaux I, 351, Cours de la Libération, 33405 Talence, France

Received: March 24, 2006; In Final Form: May 10, 2006

We have investigated the infrared (IR) vibrational spectra of acetaminophen (N(4-hydroxyphenyl) acetamide or paracetamol) complexes formed with ethanol and acetone in relation to the nature of the specific intermolecular interactions involved in the stabilization of the complexes. The structures and binding energies of the complexes have been determined using Hartree−Fock (HF) and DFT-B3PW91 procedures and different Pople's basis sets as well. The main results are presented and discussed by considering the hydroxyl (OH), amino (NH), and carbonyl (CO) chemical groups of acetaminophen interacting with the acetone or ethanol molecules either separately or in conjunction in the complex formation. The frequency shifts and IR intensity variations associated with the internal modes of acetaminophen (namely ν_{OH}, ν_{NH}, and ν_{CO}) as well as the most pertinent vibrational probes of ethanol (ν_{OH}) and acetone (symmetric ν_{CO} and ν_{CCC} stretching modes) interacting with acetaminophen have been analyzed. The predicted spectral changes have been critically discussed in comparison with IR absorption measurements of acetaminophen dissolved as a solute in ethanol or acetone CO_2 expanded solutions. It is argued that the exchange-correlation contribution taken into account in DFT calculations is likely significant in determining the main IR spectral features of acetaminophen complexes formed with acetone or involving hydrogen-bonded as with ethanol.

1. Introduction

During the two past decades, new alternatives have emerged for the production of micronic and submicronic crystalline particles with a narrow size distribution and others microphysical specificities (such as morphology, polymorphic nature, etc.) using compressed fluids either in liquid phase or under supercritical (SC) conditions.[1−10] In this context, CO_2-expanded solvents (liquid or dense gas) gained great interest as an ecological substitute for liquid organic solvent in a series of crystallization industrial processes due to the low toxicity and nonflammable properties of CO_2. Despite severe limitations inflicted by the low solvent power of CO_2, the use of CO_2-expanded solvents in the Depressurization of an Expanded Liquid Organic Solution (DELOS) crystallization process offers a new route toward new techniques to synthesize materials unachievable until now.[1,2,11−13] Indeed, CO_2-expanded solvents constitute homogeneous media in which the solvent organic molecules have been replaced by CO_2 (lower than 80% in volume unit). In contrast to liquid solvents, the CO_2-expanded media have a substantial higher capacity to dissolve polar and ionic compounds as the solvation power of such compressed fluids can be significantly tuned by pressure variations at a given temperature. Recent solubility measurements of well-known commercially analgesic drugs as acetaminophen (N(4-hydroxyphenyl)acetamide) or paracetamol have been carried out in ethanol/CO_2 and acetone/CO_2 mixtures.[1,2] It was found that the solubility curve of acetaminophen was strongly dependent upon the organic solvent and the evolution of the CO_2-solvent concentration. For instance, in a hydrogen-bonded solvent like ethanol, the acetaminophen solubility is slightly more pronounced than in a non-hydrogen bonding solvent like acetone as the CO_2 concentration increases.[2]

A recent investigation has been devoted to assess at the microscopic level this preferential solvation phenomenon using absorption spectrometry in the mid-infrared (MIR) domain.[1,2] It has been demonstrated that specific or nonspecific solute−solvent interactions govern such a differential solvation of acetaminophen in the cybotactic region of the two CO_2-expanded organic solvents. In others terms, dipole−dipole interactions between the carbonyl groups of acetaminophen and acetone can be more easily broken down with the increase of CO_2 in the mixture in contrast to the other system in which ethanol acts as an Hydrogen Bond Donor (HBD). Moreover, using a refined Linear Solvation Energy Relationship Analysis (LSER), it has been possible to correlate macroscopic solubility data with observed IR spectroscopic features associated with both ν_{CO} and ν_{NH} vibrational modes of acetaminophen dissolved in ethanol/CO_2 and acetone/CO_2 mixtures underlying the adequateness to use such multitechnique approaches for understanding the solvation phenomena in compressed fluids at the molecular level.

Clearly, the solvation of acetaminophen in CO_2 expanded either ethanol or acetone solvents, depending on a subtle balance between solute−solvent and solvent−solvent interactions in which additional many-body interactions can also play a role. Theoretical chemistry calculations can provide useful insights to these problems in elucidating the nature of solute−solvent interactions from the structural and energetic properties of isolated complexes in connection with their specific spectral features. In addition, the influence of many-body interactions on both structure and stabilization energy of such acetaminophen complexes can be also assessed from theoretical chemistry calculations constituting therefore a first step toward the

* Corresponding author phone: 33 5 40 00 63 59; fax: 33 5 40 00 84 02; e-mail: y.danten@lpcm.u-bordeaux1.fr.

10.1021/jp061845l CCC: $33.50
Published on Web 06/23/2006

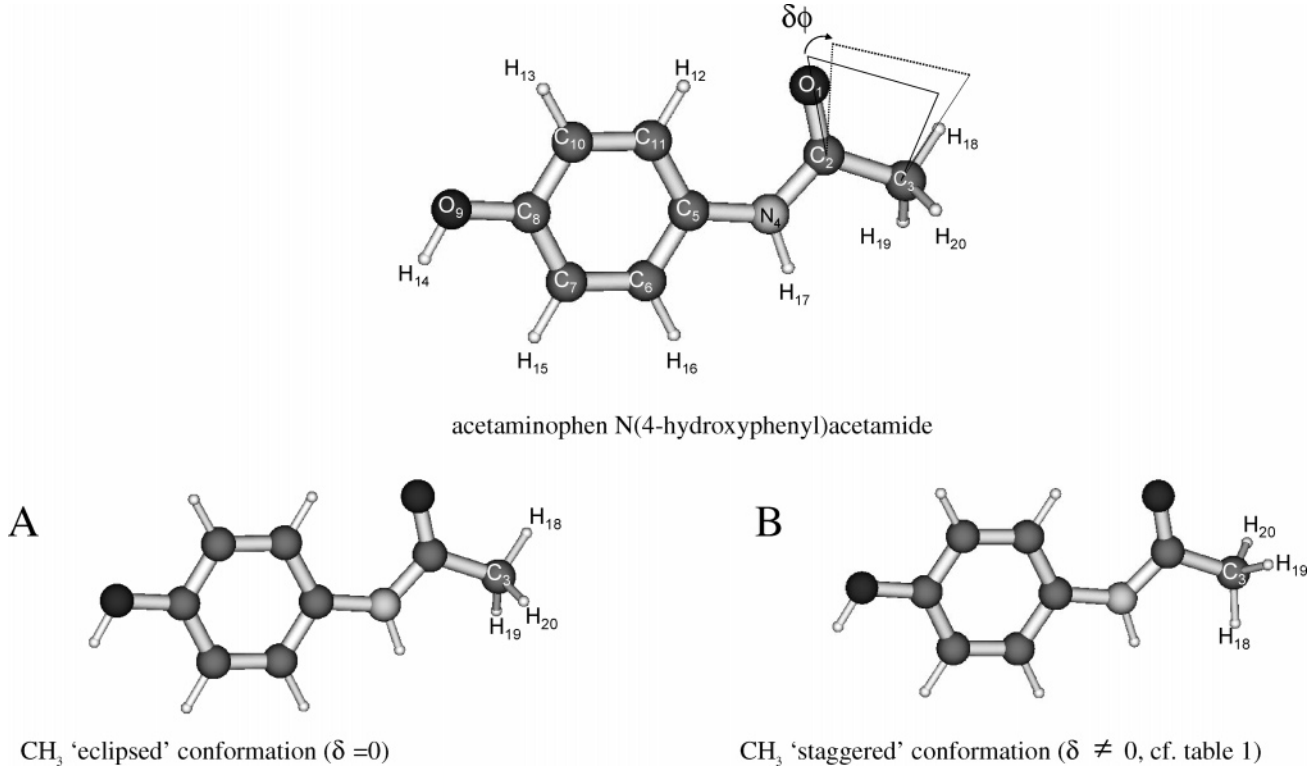

Figure 1. Schema of the acetaminophen or N(4-hydroxyphenyl)acetamide) in conformation A1[15] having (A) an 'eclipsed' methyl group (CH_3) conformation (CH bond of the CH_3 group in eclipsed configuration compared with the CO group of acetaminophen) and having (B) a 'staggered' CH_3 conformation compared with the CO bond of acetaminophen.

understanding of solvation mechanism, even if this approach mostly relies upon an energetic criterion basis.

This paper is aimed at understanding intermolecular interactions taking place in the stabilization mechanism of acetaminophen complexes formed with ethanol and with acetone. This is critically discussed in relation with the main spectral features induced under the complex formation (frequency shifts and IR intensity variations) with a particular emphasis on the ν_{OH}, ν_{NH}, and ν_{CO} vibrational modes of acetaminophen interacting with either ethanol or acetone species. For this reason we have preliminarily determined the equilibrium structure and IR spectrum of monomeric acetaminophen using HF and DFT quantum chemistry methods. Then, the global and local energy minimum structures and stabilization energies of the 1:1 and 1:3 complexes formed with a single acetaminophen molecule have been calculated, and the main IR spectral changes under the complex formation have been assessed. We have also discussed the spectral signatures obtained from the vibrational probe of the solvent, namely, the ν_{OH} stretching mode of ethanol or the antisymmetric ν_{CCC} and symmetric ν_{CO} stretching modes of acetone. Finally, spectral predictions have been compared with our IR measurements on acetaminophen in CO_2 expanded either ethanol or acetone.[1,2]

2. Methodology and Details of the Calculations

Quantum chemistry calculations have been carried out using the Gaussian-03 program.[14] The structures of the 1:1 acetaminophen complexes in which only a single of the three chemical groups interacts with the ethanol or acetone molecule as well as the structure of the 1:3 tetramer in which each of the three chemical groups of acetaminophen interacts with a moiety have been preliminarily fully optimized at the HF/6-31G level. At this computational level, all the conformations of acetaminophen interacting with either ethanol or acetone species were allowed to vary though it was always found that acetaminophen remains close to its most stable conformation (labeled A1 in ref 15) close to an 'eclipsed' conformation of the methyl (CH_3) with respect to the CO group (cf. Figure 1A). However, to assess the influence of the exchange-correlation contribution to the stabilization energy and the infrared spectral signatures of such complexes, we have carried out in a second step DFT calculations using the B3PW91 functional.[16−18] It is now well-established that the B3-based DFT procedures provide a very cost-effective mean of determining satisfactory harmonic vibrational frequencies on a series of molecules in comparison with others procedures (B-based DFT or MP2 theory of perturbation).[19] For this purpose, we have considered basis sets elaborated from the 6-31G basis set (preliminarily used at the HF level) extended by first one set of polarization d-functions [6-31G(d)] at which in a second step, diffuse sp-functions [6-31+G(d)] have been added. Finally, we have also used in the case of the DFT-B3PW91 calculations of the isolated 1:1 complexes, the triple split valence basis set with additional sp-diffuse functions and one set of polarization d-functions on heavy atoms and one set of polarization p-functions on hydrogen atoms. Again, the geometry of all the 1:1 and 1:3 complexes determined from the DFT-B3PW91 procedure have been fully optimized using the split valence 6-31G(d) and 6-31+G(d) basis sets and the triple split valence 6-311++G(d,p) basis set.[20−30] In the following of this paper, these three computational levels will be distinctly quoted as DFT1, DFT2, and DFT3, respectively. For isolated dimers (or 1:1 complexes), the calculated interaction energies (ΔE_{int}) have been have been corrected using the basis set superposition error (BSSE) by the full counterpoise (CP) technique.[31] For oligomers of higher size and in particular for tetramers (or 1:3 complexes), the BSSE corrected binding energy has been obtained according to the site−site function counterpoise method (SSFC).[32−35] Because we will be mainly

TABLE 1: Calculated Geometry Parameters (Bond Lengths, Bond Angles, and Dihedral Angles) of the Equilibrium Structure of the Acetaminophen from the DFT-B3PW91 Method Using Three Different Pople's Basis Sets (See Text)[b]

distances (Å)				angles (deg)				dihedral angles (deg)			
	DFT1	DFT2	DFT3		DFT1	DFT2	DFT3		DFT1	DFT2	DFT3
$R(O_1,C_2)$	1.222	1.224	1.217								
$R(C_2,C_3)$	1.519	1.517	1.515	$\alpha(O_1,C_2,C_3)$	121.3	121.3	121.5				
$R(N_4,C_2)$	1.372	1.372	1.372	$\alpha(N_4,C_2,O_1)$	124.2	123.9	124.0	$\delta(N_4,C_2,O_1,C_3)$	180.	180.	180.
$R(C_5,N_4)$	1.409	1.411	1.410	$\alpha(C_5,N_4,C_2)$	128.9	129.2	129.1	$\delta(C_5,N_4,C_2,O_1)$	0.	0.	0.
$R(C_6,C_5)$	1.400	1.400	1.397	$\alpha(N_4,C_5,C_6)$	117.7	117.6	117.6	$\delta(C_6,C_5,N_4,C_2)$	180.	180.	180.
$R(C_7,C_6)$	1.391	1.392	1.388	$\alpha(C_7,C_6,C_5)$	121.0	121.0	121.0	$\delta(C_7,C_6,C_5,N_4)$	180.	180.	180.
$R(C_8,C_7)$	1.396	1.396	1.393	$\alpha(C_8,C_7,C_6)$	120.0	119.9	120.0	$\delta(C_8,C_7,C_6,C_5)$	0.	0.	0.
$R(O_9,C_8)$	1.364	1.367	1.365	$\alpha(O_9,C_8,C_7)$	123.0	123.0	122.9	$\delta(O_9,C_8,C_7,C_6)$	180.0	180.0	180.0
$R(C_{10},C_8)$	1.396	1.395	1.392	$\alpha(C_{10},C_8,O_9)$	117.8	117.7	119.3	$\delta(C_{10},C_8,C_7,C_6)$	0.	0.	0.
$R(C_{11},C_{10})$	1.389	1.391	1.388	$\alpha(C_{11},C_{10},C_8)$	120.9	120.9	120.9	$\delta(C_{11},C_{10},C_8,C_7)$	0.	0.	0.
$R(H_{12},C_{11})$	1.082	1.082	1.080	$\alpha(H_{12},C_{11},C_5)$	119.2	119.5	119.4	$\delta(H_{12},C_{11},C_5,N_4)$	0.	0.	0.
$R(H_{13},C_{10})$	1.086	1.086	1.084	$\alpha(H_{13},C_{10},C_8)$	118.8	119.0	120.2	$\delta(H_{13},C_{10},C_8,O_9)$	0.	0.	0.
$R(H_{14},O_9)$	0.967	0.968	0.961	$\alpha(H_{14},O_9,C_8)$	108.9	109.7	109.5	$\delta(H_{14},O_9,C_8,C_{10})$	180.0	180.0	180.0
$R(H_{15},C_7)$	1.089	1.089	1.087	$\alpha(H_{15},C_7,C_8)$	120.4	120.5	120.4	$\delta(H_{15},C_7,C_8,O_9)$	0.	0.	0.
$R(H_{16},C_6)$	1.089	1.089	1.087	$\alpha(H_{16},C_6,C_5)$	120.0	120.1	120.0	$\delta(H_{16},C_6,C_5,N_4)$	0.	0.	0.
$R(H_{17},N_4)$	1.010	1.010	1.008	$\alpha(H_{17},N_4,C_2)$	116.2	116.1	116.0	$\delta(H_{17},N_4,C_2,O_1)$	180.	180.	180.
$R(H_{18},C_3)$	1.095	1.095	1.093	$\alpha(H_{18},C_3,C_2)$	114.6	114.4	114.4	$\delta(H_{18},C_3,C_2,O_1)$	180.	180.	180.
$R(H_{19},C_3)$	1.095[a]	1.095[a]	1.092[a]	$\alpha(H_{19},C_3,C_2)$	108.6[a]	108.6[a]	108.5[a]	$\delta(H_{19},C_3,C_2,O_1)$	−58.1[a]	−58.2[a]	−58.2[a]
$R(H_{20},C_3)$	1.095[a]	1.095[a]	1.092[a]	$\alpha(H_{20},C_3,C_2)$	108.6[a]	108.6[a]	108.5[a]	$\delta(H_{20},C_3,C_2,O_1)$	58.1[a]	58.2[a]	58.2[a]

[a] Using the DFT-B3PW91 procedure, the equilibrium structure of acetaminophen is found having C_s symmetry. Thus, the $R(H_{19},C_3)$ and $R(H_{20},C_3)$ bond distances and the $\alpha(H_{19},C_3,C_2)$ and $\alpha(H_{20},C_3,C_2)$ angles are identical, while the $\delta(H_{19},C_3,C_2,O_1)$ and $\delta(H_{20},C_3,C_2,O_1)$ dihedral angles have values identical but of opposite sign. [b] DFT1 = B3PW91/6-31G*, DFT2 = B3PW91/6-31+G*, and DFT3 = B3PW91/6-311++G**.

concerned with IR spectra changes of acetaminophen under complex formation with ethanol or acetone species, we have carried out a further vibrational analysis of these different complexes using the standard Wilson FG matrix formalism based on the harmonic force field approximation.[36] The vibrational frequencies (including low-frequency modes) and IR activities variations due to the complex formation have been calculated for all the optimized structures of the acetaminophen complexes.

3. Acetaminophen Monomer

3.1. Equilibrium Structure. The geometry of the acetaminophen monomer has been optimized without symmetry restrictions. However, it is noteworthy that the hydroxyl (OH) group is constrained to hold on to, more or less, a trans conformation with respect to the carbonyl (CO) function which corresponds with the lowest energy conformation of the monomer of interest here.[15] At the HF/6-31G computational level, the most stable structure is found with the quasi planar conformation A1 (Figure 1) according to the nomenclature used in ref 15. In this equilibrium structure, the acetaminophen monomer differs by a dihedral angle deviation $\delta\Phi$ of 16.1° from the planar geometry (C_s symmetry) in which a CH bond of the methyl (CH_3) group should be found with an 'eclipsed' conformation with respect to the CO bond ($\delta\Phi = 0$, Figure 1A) In this latter CH_3 'eclipsed' conformation, the total electron energy of acetaminophen only differs by 4.8×10^{-3} mH from the value corresponding to the equilibrium structure. Whereas in the CH_3 'staggered' conformation (planar geometry having a C_s symmetry, cf. Figure 1B), the total electron energy is greater by 0.1 mH (<0.1 kcal/mol) than that of the equilibrium structure even if the overlap between the orbitals of the CH_3 protons with those of the O-atom of the CO group is now minimized. Thus, the rotational barrier of the CH_3 group is predicted quite low at the HF/6-31G level.

Using the DFT-B3PW91 method in conjunction with the Pople's basis sets (namely, the double split valence 6-31G(d) and 6-31+G(d) basis sets (DFT1 and DFT2 computational levels, respectively) and the triple split valence 6-311++G-(d,p) basis set (DFT3)), the most stable structure of the acetaminophen monomer is again found having a planar structure (C_s symmetry) in which a CH bond of its CH_3 group is now in a 'staggered' conformation with respect to the bond of the CO group (Figure 1B). The calculated bond distances, angles, and dihedral angles of the equilibrium structure of the acetaminophen are found quite similar using both double split valence basis sets as well as the triple split valence basis set (Table 1) although with using this latter basis set the bond lengths of the OH, NH, and CO groups are found slightly shorter respectively than using the double split valence ones. The calculated bond lengths, angles, and dihedral angles of the equilibrium structure of the acetaminophen monomer have been gathered in Table 1.

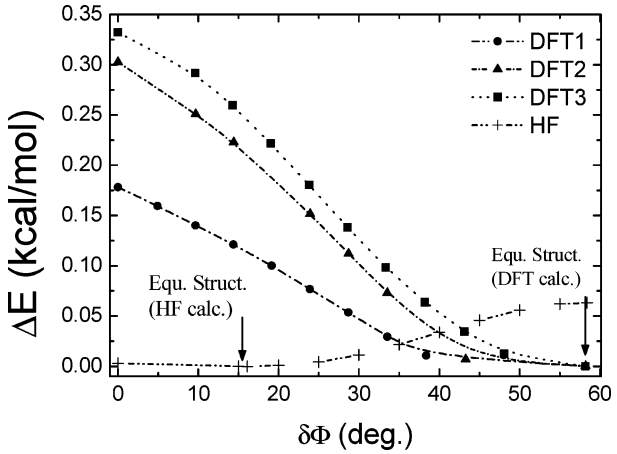

Figure 2. Evolution of the Potential Energy Surface (PES) with the dihedral angle deviation $\delta\Phi$ ($\delta\Phi = 0$ being an 'eclipsed' CH_3 conformation) associated with the rotational motion of the CH_3 group calculated at the HF/6-31G level (dash dot dot line) and using the DFT-B3PW91 procedure with the 6-31G* = DFT1 (circle dash dot line), 6-31+G** = DFT2 (triangle dash dot line), and 6-311++G** DFT3 (square dot line) Pople's basis sets.

The evolution of the DFT-B3PW91 calculated Potential Energy Surface (PES) with the dihedral angle $\delta\Phi$ associated with the rotational motions of the CH_3 group of the acetaminophen monomer (Figure 1) is displayed in Figure 2 and compared with that evaluated at the HF/6-31G level. Clearly, the predicted conformation and the rotational barrier estimates

TABLE 2: Predicted Frequencies and IR Intensities Associated with the Stretching Modes of the OH, NH, and CO Chemical Functions and the CH Stretching Modes of the CH_3 Group and the Phenol Ring of Acetaminophen in the Optimized Structure from the HF and DFT-B3PW91 Methods[a]

	frequency transition ν (cm^{-1})					IR intensity I_{IR} (km/mol)					
	exp.[15 b]	HF	DFT1	DFT2	DFT3	exp.[15 b]	HF	DFT1	DFT2	DFT3	approximated assignment
					acetaminophen monomer						
$\nu_{C=O}$	1678(1722)	1875.5	1803.7	1776.3	1767.4	99.3	189.7	234.3	281.0	287.3	CO group (mixed)
ν_s(CH)	2855	3204.4	3072.0	3069.3	3051.4	2.8	6.9	10.0	12.0	9.7	CH stretches of the CH_3
ν_a(CH)	2928	3270.9	3155.4	3151.4	3133.7	14.9	15.3	17.3	16.3	15.3	group
	3010	3333.0	3159.0	3155.5	3134.9	5.9	5.8	4.1	3.0	3.4	
ν_{PhH}(CH)	ranging from 2960	3341.5	3173.4	3172.3	3156.8		21.0	21.0	21.1	18.6	CH stretching modes of the
	to 3160 cm^{-1}	3364.0	3190.8	3189.5	3173.8		19.2	17.4	16.5	11.2	phenol ring
		3402.7	3224.2	3221.1	3201.6		4.1	5.3	4.9	3.2	
		3460.2	3276.9	3270	3246.1		5.3	5.6	5.8	7.5	
ν_{NH}	3440(3466)	3876.9	3640.0	3636.6	3647.5	21.4	30.0	16.2	17.2	21.1	NH group
ν_{OH}	3594(3654)	4049.3	3791.1	3788.3	3867.5	41.3	74.2	56.4	64.1	78.7	donor OH_group
					ethanol monomer						
ν_{OH}	3660.8	4029.3	3794.2	3796.0	3875.5	18.4	23.6	14.2	23.6	30.6	OH stretch
					acetone monomer						
ν^s_{CO}	1730.	1904.6	1839.0	1814.2	1805.3	115.	176.9	157.2	199.8	210.7	CO stretch
ν^a(CCC)	1218.	1379.6	1249.7	1249.4	1236.73	46.	86.3	73.9	72.0	67.5	CCC stretch

[a] The same for ethanol and acetone species under their monomeric form. It is noteworthy that no symmetry has been reported with the assignment of the antisymmetric stretching mode of the methyl (CH_3) group of acetaminophen. The most intense band associated with both antisymmetric stretches is observed at higher frequencies in liquid $CDCl_3$. [b] Values in parentheses correspond with measured frequencies in the gaseous phase reported in ref 40 (see text and Figure 3).

of the CH_3 group radically differ. Using the DFT-B3PW91 method, the equilibrium structure is now energetically quite separated from the CH_3 'eclipsed' conformation (transition state) by a rotational barrier ranging from 0.2 to 0.3 kcal/mol using the different Pople's basis sets. This result emphasizes the influence of the exchange-correlation contribution introduced through the B3PW91 function in the DFT calculations, whereas at the HF/6-31G level the rotational motions of the CH_3 group are found quasi-free (no rotational barrier).

3.2. IR Spectrum of Acetaminophen Monomer. At the HF/6-31G level, the vibrational analysis (frequency and IR intensity of each internal mode) of acetaminophen in the equilibrium geometry (conformation A1) is in agreement with the predicted IR spectrum obtained in a previous study.[15] However, we notice numerical deviations which are mainly due to the different softwares used in both works. The ν_{OH} and ν_{NH} bands of acetaminophen are situated at the harmonic frequencies of 3876.9 and 4049.3 cm^{-1} with IR intensity values of 74.2 and 30 km/mole (modes 1 and 2 labels in ref 15), whereas the $\nu_{C=O}$ band associated with the CO group (amide 1) is predicted at 1875.5 cm^{-1} with an IR intensity of 189.7 km/mole (cf. Table 2). It is noteworthy that the ν_{CO} mode is mixed with both δ_{CNH} and δ_{OCN} deformation modes.[15] Because electron correlation and vibrational anharmonicity have been neglected in the standard Wilson's vibrational analysis,[36] the predicted frequencies are usually overestimated compared with the fundamental experimental ones. Scaling factors have been reported in the literature[19,37,38,39] in order to take into account such effects and to facilitate comparison with experimental observed frequencies especially available from IR measurements in gaseous phase.[40] At the HF/6-31G level, the frequency scaling factor is 0.8929.[39]

The frequency and IR intensity values associated with the ν_{OH}, ν_{NH}, and ν_{CO} vibrational modes of acetaminophen calculated from the DFT-B3PW91 procedure using double and triple split valence basis sets have been also reported in Table 2 and compared with both HF/6-31G calculations and IR measurements in liquid $CDCl_3$.[15] It comes out that by taking into account the exchange-correlation contribution, the frequencies of these fundamental transitions are lower than those calculated at the HF/6-31G level even overestimating the experimental ones. The

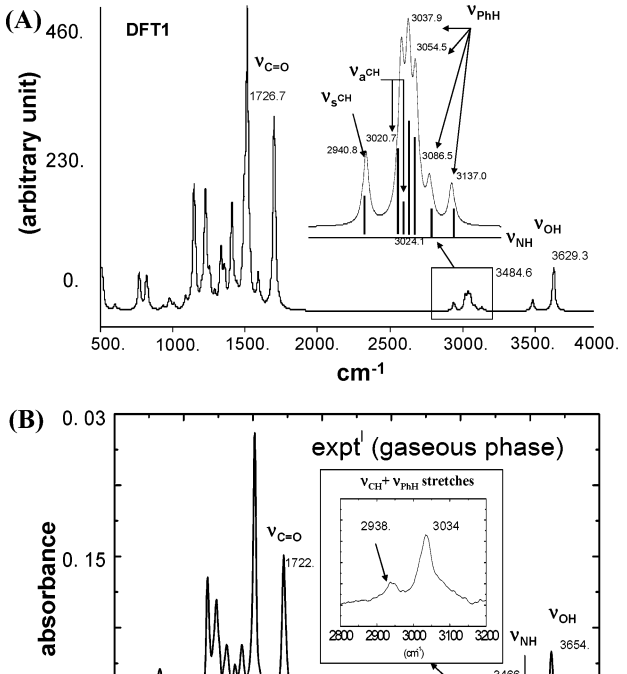

Figure 3. Comparison between the IR measurements of acetaminophen in gaseous phase[40] with the calculated IR spectrum using the DFT-B3PW91 procedure. In this figure, the calculated IR lines have an arbitrary width of 5 cm^{-1}, and the scale factor is of 0.9573 at the DFT1 level.[19,39]

intensity of the ν_{CO} mode is again found greater than the experimental value (in liquid $CDCl_3$) and in the HF calculations (cf. Table 2). Moreover, the ratio of the intensity values of the ν_{OH} mode over the ν_{NH} one is 3.5−3.7 i.e., slightly greater than the value 2.5 calculated at the HF/6-31G level (instead of 1.9 in liquid $CDCl_3$[15]).

We compare in Figure 3 the IR spectrum at the scaled frequencies calculated at the DFT1 level with the IR measurements of acetaminophen in gaseous phase.[40] At this computa-

tional level, the frequency scaling factor has been previously reported as 0.9573.[19] In this figure, the predicted IR bands are supposed having Lorentzian profiles with an arbitrary full width of 5 cm^{-1} which corresponds approximately with the resolution of the measured IR spectrum of acetaminophen in gaseous phase. It is noteworthy that the measured frequencies in the gaseous phase (as assigned) have been also reported in Table 2 (values in parentheses) and compared with the experimental values measured for acetaminophen diluted in liquid $CDCl_3$ reported in ref 15.

In the gaseous phase, the ν_{OH} and ν_{NH} bands of acetaminophen are found at the frequencies of 3654 and 3466 cm^{-1}, respectively, and the ν_{CO} band at about 1722 cm^{-1} (Table 2). It comes out that these frequencies are found to be systematically higher than those measured in liquid $CDCl_3$ (Table 2 and ref 15). This is mainly due to perturbations induced by the interactions of acetaminophen with the surrounding $CDCl_3$, molecules leading to a shift toward lower frequencies compared with those in the gaseous phase.

We have also calculated the frequency and IR intensity associated with the CH stretching modes of the CH_3 group (Table 2). At the HF/6-31G level, the IR line associated with the symmetric ν_s(CH) stretching mode is evaluated at the lowest frequency value of 3204 cm^{-1}, whereas the vibrational transition of the two antisymmetric ν_a(CH) stretching modes are found at frequencies of 3271 and 3333 cm^{-1} (not scaled), respectively. The most intense band of these three stretching vibrations is associated with the ν_a(CH) mode situated at the lowest frequency value. Notice that the calculated intensity of the ν_s(CH) and ν_a(CH) modes are found relatively close to those measured for acetaminophen in $CDCl_3$ liquid.[15] The predicted IR band of the ν_{PhH}(CH) stretching modes of the CH bonds of the phenol ring are found in the spectral range 3340−3460 cm^{-1} (not scaled) i.e., at frequencies greater than those of the ν_s(CH) and ν_a(CH) modes. It is noteworthy that from the IR measurements in liquid $CDCl_3$, the ν_s(CH) mode of acetaminophen (∼2855 cm^{-1}) is found well-separated from the two ν_a(CH) modes situated at about 2928 and 3010 cm^{-1}. The later one is overlapping with the broad composite profile due to the ν_{PhH}(CH) stretches of the phenol ring at 3000−3100 cm^{-1}.[15] Thus, the observed intense band at 2928 cm^{-1} should be attributed with that corresponding to the two ν_a(CH) modes of acetaminophen. This is consistent with the IR measurements of gaseous phase acetamide (C_2H_5NO) for which the ν_s(CH) and ν_a(CH) modes are assigned and found at 2860 and 2967 cm^{-1}, respectively.[41] Therefore, the IR band of the ν_s(CH) mode (at 2855 cm^{-1} in liquid $CDCl_3$) should be not observed on the measured spectrum of acetaminophen in the gaseous phase.[40]

Using the DFT-B3PW91 procedure, the frequency position of the ν_s(CH) vibrational transition (situated at the lowest frequency) is again well-separated from the two ν_a(CH) stretching modes. The most intense ν_a(CH) band is situated at the lowest frequency position of the doublet structure formed with the second less intense ν_a(CH) band. The calculated IR bands associated with both the higher frequency ν_a(CH) mode and the ν_{PhH}(CH) stretches associated with the phenol ring are found in the region of 3100−3300 cm^{-1} (not scaled). However, the two ν_a(CH) modes which were found to form a well-defined doublet structure at the HF/6-31G level (spectral separation of 62 cm^{-1}) are found only separated by a few wavenumbers using the DFT-B3PW91 procedure. This significant difference between the HF and DFT-B3PW91 spectral features of the ν_a(CH) modes is closely related to the distinct CH_3 conformations of isolated acetaminophen. In particular, this is due to the charge distribution of the hyperconjugated bonds of the chemical functional CH_3, CO, and NH groups which drastically differs by considering the exchange-correlation contribution in the DFT calculations. Unfortunately, it is not possible to validate definitively the adequateness of the use of the DFT-B3PW91 procedure compared with the HF method from the measured IR spectrum in the region of the ν_s(CH), ν_a(CH), and ν_{PhH}(CH) stretches of acetaminophen in the gaseous phase (2800−3200 cm^{-1}) which is not unambiguously assigned in the spectral range (band observed at about 2938 cm^{-1}) as mentioned before. Because the DFT calculations take into account the exchange-correlation contribution and that in particular this leads to a non-negligible rotational barrier of the CH_3 group of acetaminophen, we have decided in the following to investigate the properties of acetaminophen complexes using the DFT-B3PW91 method.

Then, we shall discuss the structure and the IR spectra of the complexes of acetaminophen formed with ethanol or acetone. For this purpose, we have determined the optimized structures of such complexes using the DFT-B3PW91 procedure and the double and triple split valence Pople's basis sets previously mentioned. The structures and binding energies calculated at the HF/6-31G level will be first provided to illustrate the influence of the electron exchange-correlation on the structure and stabilization energy of the 1:1 complexes of acetaminophen formed with ethanol or acetone. Only the most relevant calculated structural parameters i.e., internal bonds lengths of the hydroxyl (OH), amino (NH), and carbonyl (CO) chemical functions of acetaminophen, the intermolecular distances and relative angles between the moieties, and the values of the binding energy are provided from the different computational methods. However, a full list of calculated structural parameters for the distinct complexes may be obtained from the authors upon request. In a second step, the predicted frequency shifts and IR intensity variations under the complex formation associated with the relevant internal modes of acetaminophen will be mainly discussed on the basis of the results obtained from the DFT-B3PW91 procedure in view of the satisfactory agreement obtained between the calculated scaled frequencies with those measured in IR for isolated acetaminophen.[40] Nevertheless, HF calculations have been sometimes reported in tables for the purpose of the discussion, and further details about the calculated spectral properties of these complexes can be again obtained from the authors upon request.

4. Acetaminophen Complexes Formed with Ethanol

4.1. Structures and Binding Energies of the Dimer. Using both HF and DFT-B3PW91 methods, we found three distinct (global and local energy minimum) structures for the 1:1 acetaminophen-ethanol complex (Figures 4 and 5). A brief survey of the calculated geometrical parameters reported in Table 3 shows that the values of bond lengths, intermolecular distances, and relative angles are found quite comparable for the HF and DFT-B3PW91 calculations. For this reason, we will use the same nomenclature to label the different structures of the 1:1 complex obtained from the two distinct methods even if the exchange-correlation contribution introduces significant deviations upon the evaluation of their binding energy.

The most stable structure of the 1:1 complex is found with ethanol interacting with the OH group of acetaminophen (Figure 4). In this structure (D1), the proton of the OH group of the phenol ring of acetaminophen forms a quasi-linear O−H···O (1.80 Å ≤ R_O···HO ≤ 1.83 Å) hydrogen bond with the O atom of ethanol which plays the role of a Hydrogen Bonded Acceptor (HBA). From DFT-B3PW91 calculations, it is found that the

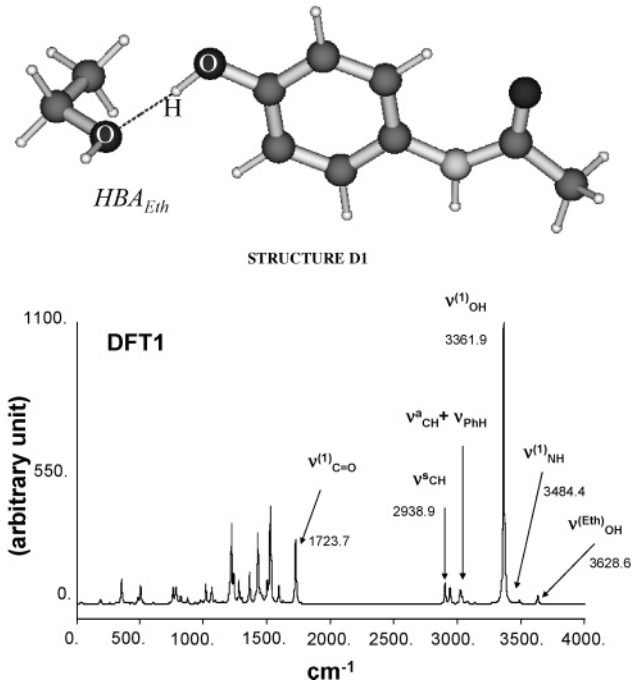

Figure 4. Calculated IR spectrum at the scaled frequencies of the 1:1 acetaminophen complex formed with ethanol in the equilibrium structure D1 at the DFT1 level (scale factor given in legend of Figure 3). The width of the calculated IR profiles has an arbitrary width of 5 cm^{-1}.

relative angle $\alpha_O\cdots HO(1)$ formed between the two moieties is sparingly dependent on the basis sets used ($171° \leq \alpha_O\cdots HO(1) \leq 173°$) and that the CH_3 conformation of acetaminophen is weakly varied from its 'staggered' conformation under complex formation (dihedral angle deviation less than 0.17°).

However, the equilibrium structure of the 1:1 complex is found less stable from the DFT calculations than that calculated at the HF/6-31G level (~ -8.9 kcal/mol) with an interaction energy $\Delta E_{int}^{(cor)}$ (BSSE corrected) varying from -7.0 to -6.4 kcal/mol (see Table 3). This results from the exchange-correlation contribution provided through the Perdew/Wang (nonlocal correlation) functional (B3PW91).[16−18] The BSSE contribution to the total interaction energy gradually decreases with the quality of the basis set used. Thus, the BSSE energy correction reaches comparable values of $+0.9$ and $+0.7$ kcal/mol using the 6-31+G* (DFT2) and 6-311+G** (DFT3) basis sets, respectively.

We found two other secondary structures for the 1:1 complex (local energy minima). In the first structure (D2), the O-atom (HBA) of ethanol interacts with the proton of the NH group of acetaminophen leading to a quasi-linear N−H···O intermolecular bond (Figure 5A) with a calculated distance $R_O\cdots HN$ ranging from 2.0 to 2.1 Å (Table 3). As for structure D1, the CH_3 conformation of acetaminophen is weakly affected under the complex formation (dihedral angle deviation less than 3.0°). In this structure, the BSSE corrected binding energy $\Delta E_{int}^{(cor)}$ is -4.5 kcal/mol by taking into account the exchange-correlation contribution included in the DFT calculations (instead of -7.0 kcal/mol at the HF/6-31G level).

Finally, in structure (D3) the O-atom of the CO group (proton acceptor center) interacts with the hydroxyl proton of ethanol which plays the role of a Hydrogen Bonded Donor (HBD) (Figure 5B) and the interatomic distance $R_H\cdots OC$ ranges from 1.88 to 1.93 Å (Table 3). Moreover, under the complex formation, the CH_3 conformation is deviated by a dihedral angle ranging from 5.3° (DFT2) to 11.9° (DFT3). The BSSE corrected binding energy $\Delta E_{int}^{(CP)}$ is ranging from -5.8 to -5.5 kcal/mol from the DFT calculations (instead of -6.8 kcal/mol at

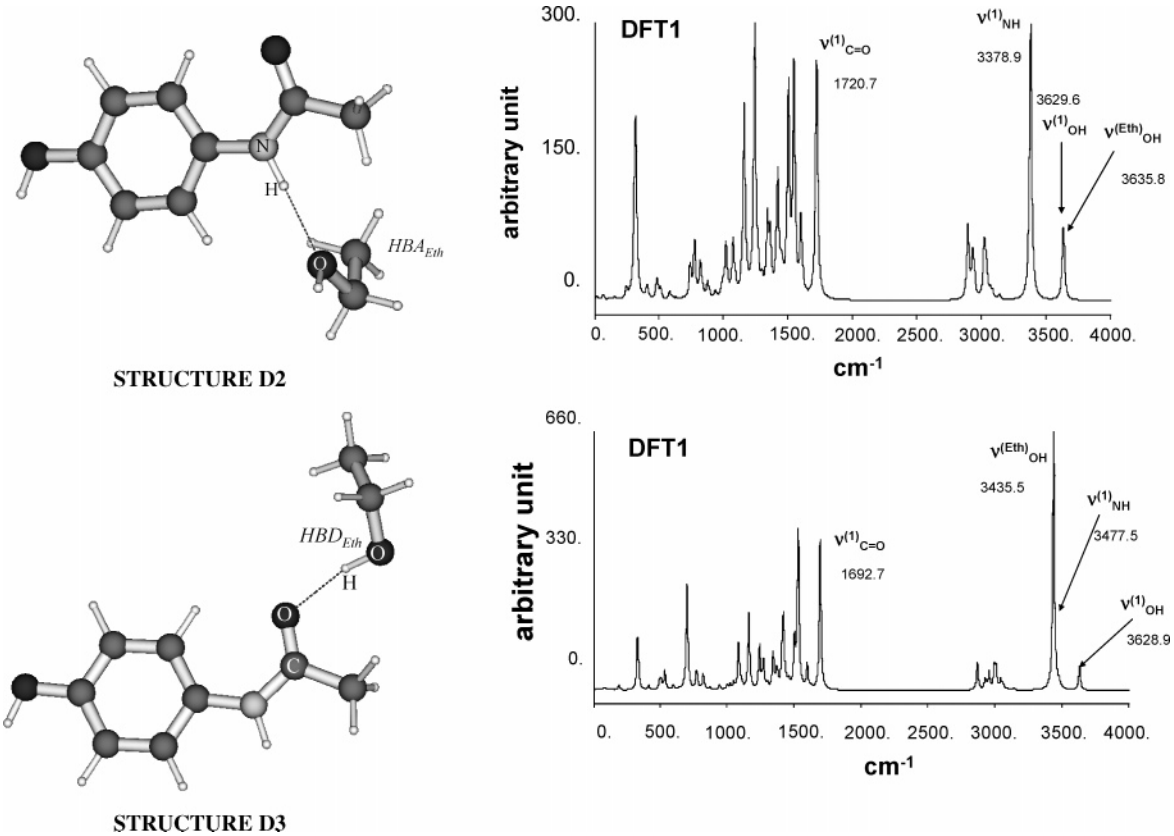

Figure 5. Calculated IR spectra (scaled frequencies) of the 1:1 acetaminophen complex formed with ethanol in structures D2 and D3 (local energy minima) at the DFT1 level. The frequency scale factor and arbitrary width are identical as previous figures.

TABLE 3: Calculated Geometrical Parameters and Interaction Energies in Global and Local Energy Minimum Structures of the Acetaminophen-Ethanol Dimer Using Both HF and DFT-B3PW91 Methods[a]

acetaminophen-ethanol dimers: structural parameters[b] and binding energies[c,d]												
	structure D1 [Eth...HO(**1**)]				structure D2 [Eth...NH(**1**)]				structure D3 [Eth...CO(**1**)]			
	HF	DFT1	DFT2	DFT3	HF	DFT1	DFT2	DFT3	HF	DFT1	DFT2	DFT3
$d^{(2)}_{OH}$ (Å)	0.95	0.97	0.97	0.96	0.95	0.97	0.97	0.96	0.96 ($+1.10^{-2}$)	0.98 ($+1.10^{-2}$)	0.98 ($+1.10^{-2}$)	0.97 ($+1.10^{-2}$)
$d^{(1)}_{OH}$ (Å)	0.96 ($+1.10^{-2}$)	0.97 ($+1.10^{-2}$)	0.98 ($+1.10^{-2}$)	0.97 ($+1.10^{-2}$)	0.95	0.97	0.97	0.96	0.95	0.97	0.97	0.96
$d^{(1)}_{NH}$ (Å)	0.99	1.01	1.01	1.01	1.00 ($+1.10^{-2}$)	1.02 ($+1.10^{-2}$)	1.02 ($+1.10^{-2}$)	1.02 ($+1.10^{-2}$)	0.99	1.01	1.01	1.01
$d^{(1)}_{CO}$ (Å)	1.23	1.22	1.22	1.22	1.23	1.22	1.22	1.22	1.24 ($+1.10^{-2}$)	1.23 ($+1.10^{-2}$)	1.23 ($+1.10^{-2}$)	1.23 ($+1.10^{-2}$)
$R_O\cdots HO$ (Å)	1.81	1.80	1.82	1.83								
$\alpha_O\cdots HO(1)$	177.5	173.2	171.4	172.8								
$R_O\cdots HN$ (Å)					2.01	2.01	2.04	2.05				
$\alpha_O\cdots HN(1)$					178.4	174.8	172.9	175.1				
$R_H\cdots OC$ (Å)									1.93	1.88	1.88	1.89
$\alpha_O\cdots OH(2)$									161.4	162.3	169.4	165.1
$\Delta E_{int}^{(cor)}$	−8.9	−7.0	−6.6	−6.4	−7.0	−4.5	−4.4	−4.5	−6.8	−5.5	−5.8	−5.7
$\Delta E_{int}^{(BSSE)}$	+1.4	+2.2	+0.9	+0.7	+1.7	+2.4	+0.6	+0.6	+1.3	+2.9	+0.5	+0.2
$\Delta E_{int}^{(ZPE)}$	+1.6	+1.4	+1.4	+1.5	+1.5	+1.1	+0.9	+1.1	+1.5	+1.5	+1.2	+1.1

[a] BSSE and ZPE contributions to the binding energy have been also reported in this table for each of the dimer structures investigated. HF = HF/6-31G, DFT1 = B3PW91/6-31G*, DFT2 = B3PW91/6-31+G*, DFT3 = B3PW91/6-311++G**. Abbreviations in this table: eth, ethanol solvent molecule; OH(**1**), acetaminophen hydroxyl group; NH(**1**), acetaminophen amino group; and OC(**1**), acetaminophen carbonyl group. [b] Significant bond length deviations of OH, NH, and CO functional groups from an isolated acetaminophen monomer have been reported and are shown in parentheses. [c] The binding energy $\Delta E_{int}^{(cor)}$ values in this table are corrected from BSSE according to the generalized Boys−Bernardi scheme. [d] Energy unit (kcal/mol).

the HF/6-31 G, see Table 3). For all the structures of the 1:1 complex, the BSSE and ZPE contributions to the total interaction energy have been reported in Table 3. At the DFT2 and DFT3 levels, the BSSE contribution to the interaction energy for both secondary structures is found quite comparable.

Using the DFT-B3PW91 procedure, the dimer D3 corresponds to the structure having intermediate interaction energy, whereas the structure D2 has the lowest binding energy (Table 3). In other terms, the exchange-correlation electron contribution (included in the DFT calculations) significantly decreases the stabilization energy of the secondary structures of the 1:1 complex of acetaminophen formed with ethanol leading to permute on the basis of an energetic criterion, the hierarchic order of both local energy minimum structures D2 and D3. However, according to both HF and DFT-B3PW91 methods, the most stable structure always corresponds with D1. For the sake of simplicity, only the results obtained from the DFT calculations will be discussed in the following.

4.2. Predicted IR Spectra of the 1:1 Complex. *Structure D1 (Figure 4B).* We display in Figure 4 the calculated (DFT1) IR spectrum associated with the fundamental transitions of the acetaminophen-ethanol dimer in its equilibrium structure. In this figure, the calculated IR lines have an arbitrary width of 5 cm^{-1}, and the band center position is situated at the scaled harmonic frequencies (scaling factor ∼0.9573[19]). However, the harmonic frequencies and IR intensities obtained at the DFT1 level as well as those obtained using the split valence 6-31+G* (DFT2) and triple split valence 6-311++G** (DFT3) basis sets have been reported in Table 4 for the vibrational modes of the moieties which are the most sensitive to the complex formation. For the sake of completeness and to ensure that each of the local minimum energy structures have been reached, we have also reported in Table 4 the lowest calculated frequencies of the 1:1 complex. The main spectral results can be briefly summarized as follow. The hydrogen-bonded nature of the intermolecular interaction involved in the stabilization of the dimer in the most stable structure is mainly reflected on the ν_{OH} stretching mode of acetaminophen. Indeed, the predicted ν_{OH} band is significantly shifted by 270−282 cm^{-1} toward lower frequencies ('red-shift') under the complex formation, while its intensity is enhanced by about 1 order of magnitude (Table 4). The IR bands associated with the NH and CO (amide 1) modes of acetaminophen are almost unperturbed by the acetaminophen-ethanol interaction. In contrast, the ν_{OH} stretching mode of HBA ethanol is only slightly red-shifted by about 10−11 cm^{-1}, while its IR intensity is enhanced by a factor 1.5−2.5.

Structure D2 (Figure 5A). In structure D2, the intermolecular N−H···O hydrogen bonding leads to a well-defined spectral signature on the amino NH stretching mode of acetaminophen. Indeed, the ν_{NH} IR line is found red-shifted by 110−123 cm^{-1} under the complex formation with an intensity enhancement of almost an order of magnitude (Table 4 and Figure 5A). As expected, the ν_{OH} mode of acetaminophen is almost unaffected. However, its IR intensity is decreased by a few percents due to subtle charge distribution effects through couplings between motions of the carbon skeleton of the phenol ring and the internal C−N coordinate.[15] In contrast, the ν_{CO} mode (amide 1) is found weakly red-shifted by 6−8 cm^{-1} due to subtle couplings existing with the δ_{CNH} (amide 2) and δ_{OCN} deformation modes of acetaminophen.

For HBA ethanol, the DFT calculated IR intensity of the ν_{OH} mode is significantly enhanced by a factor 1.5−2.5. At the DFT2 and DFT3 levels, this mode is red-shifted by 7 to 8.5 cm^{-1} such as the ν_{OH} bands of HBA ethanol and acetaminophen are found weakly separated (Table 4). In contrast, at the DFT1 level this mode is rather shifted toward higher frequencies (almost unchanged at the HF level).

Structure D3 (Figure 5B). In structure D3, the hydrogen-bond character of the intermolecular interaction is now mainly perceived on the $\nu^{(eth)}_{OH}$ stretching mode of HBD ethanol (Table 4). Indeed, this mode is found significantly red-shifted by 206−231 cm^{-1} under the complex formation. Moreover, its IR intensity is enhanced by a factor 20 compared with isolated ethanol leading to an intensity greater by an order of magnitude than that of the ν_{OH} mode of acetaminophen (Figure 5B). In addition, the CO stretching mode is red-shifted by 28−36 cm^{-1}, while its intensity is increased by 40−60%. This intensity enhancement is significantly damped with the increasing size

TABLE 4: Vibrational Analysis of Acetaminophen-Ethanol 1:1 Complexes in Structures D1, D2, and D3 Using the DFT-B3PW91 Procedure: Calculated Vibrational Frequencies and IR Intensities of the OH, NH, and CO Stretching Modes and the CH Stretches of the CH_3 Group of Acetaminophen and the ν_{OH} Stretching Mode of Ethanol

structure D1

	DFT1						DFT2						DFT3					
low freq (cm^{-1})	17.0	28.1	39.4	41.1	50.5	67.8:	13.7	22.3	33.4	42.5	54.7	65.4	13.5	22.1	32.7	40.3	52.5	62.7
internal modes	ν (cm^{-1})			I_{IR} (km/mol)			ν (cm^{-1})			I_{IR} (km/mol)			ν (cm^{-1})			I_{IR} (km/mol)		
$\nu^{(1)}_{OC}$	1800.6			252.4			1772.3			301.6			1763.3			308.4		
ν_s(CH)	3070.5			12.3			3067.9			14.2			3050.0			11.4		
ν_a(CH)	3153.5			18.4			3149.4			17.2			3131.9			16.5		
	3157.5			4.9			3154.1			3.7			3133.6			4.2		
$\nu^{(1)}_{NH}$	3639.9			15.3			3636.3			16.4			3647.6			20.5		
$\nu^{(1)}_{OH}$	3511.8			1090.4			3517.9			1098.6			3585.1			1081.		
$\nu^{(eth)}_{OH}$[a]	3790.5			35.5			3791.1			41.4			3865.0			49.5		

structure D2

	DFT1						DFT2						DFT3					
low freq (cm^{-1})	13.9	19.0	29.0	50.3	61.6	67.3	15.0	18.6	26.4	45.9	52.1	64.7	16.5	26.2	29.7	46.3	54.2	63.4
internal modes	ν (cm^{-1})			I_{IR} (km/mol)			ν (cm^{-1})			I_{IR} (km/mol)			ν (cm^{-1})			I_{IR} (km/mol)		
$\nu^{(1)}_{OC}$	1797.5			254.1			1768.4			298.8			1759.2			309.2		
ν_s(CH)	3072.7			10.5			3070.0			12.1			3051.5			10.1		
ν_a(CH)	3151.3			6.7			3148.0			5.1			3128.3			5.6		
	3164.9			11.2			3159.9			12.6			3141.3			10.4		
$\nu^{(1)}_{NH}$	3529.6			294.2			3526.8			274.8			3524.6			284.2		
$\nu^{(1)}_{OH}$	3791.5			50.2			3789.0			58.0			3868.7			71.8		
$\nu^{(eth)}_{OH}$[b]	3797.9			33.9			3793.1			36.1			3867.6			30.6		

structure D3

	DFT1						DFT2						DFT3					
low freq (cm^{-1})	16.1	25.9	30.8	52.0	71.0	82.1	9.9	17.5	25.1	44.7	59.8	67.3	12.6	19.3	25.3	41.1	63.1	73.7
internal modes	ν (cm^{-1})			I_{IR} (km/mol)			ν (cm^{-1})			I_{IR} (km/mol)			ν (cm^{-1})			I_{IR} (km/mol)		
$\nu^{(1)}_{OC}$	1768.2			381.5			1747.6			414.8			1738.1			411.75		
ν_s(CH)	3063.2			13.9			3072.9			8.7			3048.8			9.1		
ν_a(CH)	3138.2			13.2			3152.9			10.7			3122.7			11.7		
	3172.2			4.2			3163.2			5.7			3147.8			1.9		
$\nu^{(1)}_{NH}$	3632.6			17.4			3635.6			17.2			3644.2			59.6		
$\nu^{(1)}_{OH}$	3790.7			60.9			3787.7			68.6			3668.8			83.5		
$\nu^{(eth)}_{OH}$[c]	3588.3			659.2			3590.1			819.4			3640.5			742.4		

of the basis sets used (cf. values at the DFT2 and DFT3 levels). Therefore, the IR bands associated with the $\nu^{(eth)}_{OH}$ mode of HBD ethanol and the ν_{NH} mode of acetaminophen are found separated by at least 20 cm^{-1} (Figure 5B). We notice that the very intense ν_{OH} band of HBD ethanol is now predicted at a lower frequency position than that of the ν_{NH} band; a finding in marked contrast to the HF predictions.

Finally, it comes out that the exchange-correlation electron contribution considered in the DFT calculations through the B3PW91 functional plays a significant role by determining specific spectral features of the ν_a(CH) modes of acetaminophen interacting with ethanol, especially on the spectral separation changes under the complex formation. This finding is obviously related to the perturbations of the CH_3 conformation which radically differ in the three dimer structures investigated (see above). From the DFT-B3PW91 calculations, the IR lines of the two ν_a(CH) modes, initially separated by only a few wavenumbers for isolated acetaminophen, significantly move away from each other under the complex formation with ethanol (dimer structures D1 and D3) although the most intense band of the doublet structure remains located at the lowest frequency. In dimer structure D2, the most intense ν_a(CH) band corresponds with the higher frequency IR band even if their spectral separation is again decreased. In structure D1, the ν_s(CH) and ν_a(CH) stretching modes are slightly red-shifted by about 1−3 cm^{-1} (Table 4).

4.3. Acetaminophen•(Ethanol)$_3$ Tetramer. *4.3.1. Structure and Binding Energy.* We have also determined the equilibrium structure of a 1:3 complex in which each of the three ethanol molecules interacts separately with the CO, OH, and NH groups of acetaminophen. The optimized structure (labeled structure T1) is displayed in Figure 6A. The calculated structural parameters are partially gathered in Table 5. The structural arrangement of the ethanol molecules with acetaminophen appears as a quasi-superposition of the three dimer structures previously presented.

The calculated interatomic distances $R^{(1)}_O\cdots$HO (between the O-atom of acceptor ethanol interacting with the proton of the OH group), $R^{(2)}_O\cdots$HN (between the O-atom of acceptor ethanol interacting with the proton of the NH group), and $R^{(3)}_H\cdots$OC (between the proton of HBD ethanol interacting with the O-atom of the CO group), respectively, are found quite close to those reported for each of the individual dimers (D1, D2, and D3). Similarly, the computed relative angles of ethanol with respect to acetaminophen (in the tetramer) are found varied by a few degrees range from those of the dimer (cf. Tables 3 and 5). As for dimers, the exchange contribution included in the DFT-B3PW91 calculations leads to a decrease of the stabilization energy of the tetramer. Thus, the BSSE corrected total binding energy $\Delta E_{int}^{(cor)}$ ranges from −17.4 (DFT1) to −16.5 kcal/mol (DFT3) (instead of −22.8 kcal/mol at the HF level). According to the Boy-Bernardi generalized scheme,[32−35,42] the binding energy can be decomposed as a sum of irreducible 2-, 3-, and 4-bodies contributions. The main contribution results from the pair interaction energy between HBA ethanol and the OH group of acetaminophen (Table 4). Moreover, its comes out that at a given computational level, the calculated pair interaction energies between acetaminophen and either HBA ethanol (interacting

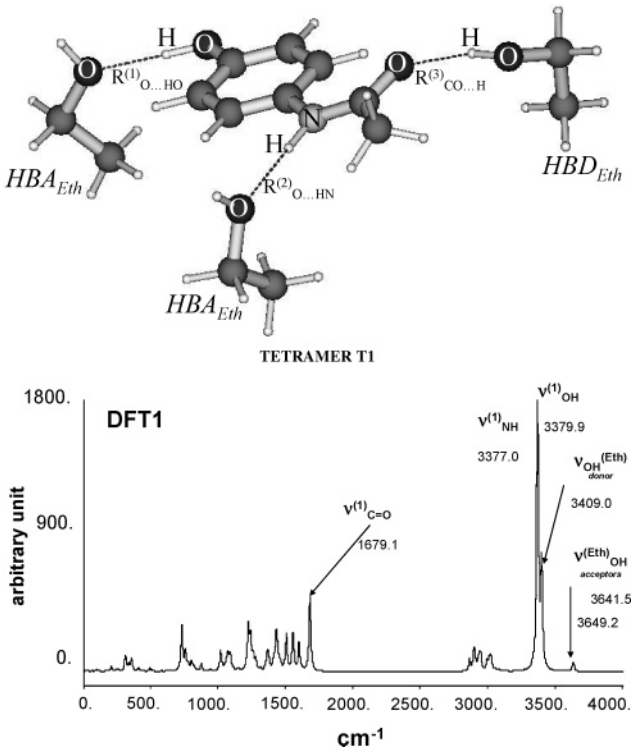

Figure 6. Calculated IR spectrum (scaled frequencies) of the 1:3 acetaminophen complex formed with ethanol in the equilibrium structure T1 at the DFT1 level.

with the OH and NH chemical groups) or HBD ethanol (with the CO group) are found close to those evaluated for each of the corresponding dimers. Thus, it can be expected that the irreducible multibodies contributions of higher order are certainly quite negligible. Indeed, it is found that the irreducible 3-bodies contribution to the total interaction energy is less than −0.3 kcal/mol, whereas the irreducible 4-bodies interaction energy can be considered as negligible (Table 5).

4.3.2. Predicted IR Spectrum (Figure 6B). The vibrational analysis of the 1:1 complex (structure T1) carried out above shows that the results obtained at the DFT3 level are quite comparable with those calculated at the DFT2 level. For this reason and for CPU time considerations as well, we have restricted our calculations of the IR spectrum of the tetramer at the DFT1 and DFT2 levels. The calculated frequency positions and IR intensities associated with the modes of acetaminophen and ethanol species sensitive to the complexation phenomenon have been reported in Table 6, and the calculated IR spectrum at scaled frequencies is displayed in Figure 6B.

Again, the hydrogen-bonded character of intermolecular interactions of the 1:3 complex in structure T1 is mainly perceived on the ν_{OH} and ν_{NH} modes of acetaminophen (interacting with the O-atom of one of the two HBA ethanol) and on the $\nu^{(eth)}_{OH}$ mode of the HBD ethanol molecules. The IR bands of the ν_{OH} modes of acetaminophen and of the HBD ethanol form a doublet structure separated by about 27−30 cm^{-1}. Under the complex formation, these two ν_{OH} stretches have been significantly red-shifted by 266−273 cm^{-1} for acetaminophen and by 246 cm^{-1} for HBD ethanol, and their intensity is enhanced by an order of magnitude. The most intense IR band is associated with the ν_{OH} stretching mode of acetaminophen and situated at the lower frequency (cf. Figure 6B and Table 6). The two IR bands of the ν_{OH} mode of HBA ethanol suffer modest spectral variations (frequency shifts and intensity enhancements) and form a doublet structure only separated by a few wavenumbers.

For the ν_{NH} mode, it is found that the tetramer formation leads to a frequency red-shift of 110−130 cm^{-1} accompanied with an intensity enhancement of about an order of magnitude (cf. Table 6). Thus, the ν_{NH} and ν_{OH} IR lines of acetaminophen are now only separated by a few wavenumbers (2.9 and 5.6 cm^{-1} at the DFT1 and DFT2 levels, respectively) though the IR intensity of the ν_{OH} mode is found greater than that of the other. The IR intensity of the ν_{CO} mode is significantly enhanced by a factor of 1.7−1.9, whereas its frequency is only red-shifted by 41−50 cm^{-1}.

5. Acetaminophen Complexes Formed with Acetone

5.1. Acetaminophen Acetone 1:1 Complex. *5.1.1. Structure and Binding Energy.* Using both HF and DFT procedures, the most stable structure (structure D′1) is found for a complex having an intermolecular O−H···O hydrogen bonding between the O-atom of the acceptor acetone (HBA) and the proton of the OH group of acetaminophen (Figure 7A). In this equilibrium structure, the interatomic distance R_O···HO is 1.83 Å from DFT calculations and the basis set size effect playing a role especially on the intermolecular relative angle (Table 7). Under the complex formation, the CH_3 (staggered) conformation of acetaminophen is slightly changed from that of the isolated monomer by a dihedral angle deviation less than 0.1°. The BSSE corrected binding energy $\Delta E_{int}^{(cor)}$ ranges from −6.8 to −7.0 kcal/mol with a BSSE contribution $\Delta E_{int}^{(BSSE)}$ varying from 0.1 to 2.3 kcal/mol. In contrast, the value of the ZPE energy contribution to the total interaction energy is found to be about 1.2−1.3 kcal/mol.

In a second local energy minimum structure (D′2), the O atom of the CO group of HBA acetone interacts with the proton of the NH group of acetaminophen (Figure 8A). The stabilization of the complex is mainly due to an intermolecular N−H···O hydrogen-bond with a R_H···O distance varying from 2.04 to 2.07 Å. The CH_3 conformation of acetaminophen is close to the 'staggered' conformation of the monomer. The BSSE corrected binding energy $\Delta E_{int}^{(cor)}$ is −4.5 to −4.8 kcal/mol with a BSSE contribution $\Delta E_{int}^{(BSSE)}$ varying from +0.3 to 2.1 kcal/mol. The ZPE correction to the total interaction energy is 1.0 kcal/mol.

At last, in the less stable structure (D′3), the CO group of acetone interacts in a head-to-tail configuration with the CO group of acetaminophen (Figure 8B). The stabilization of this 1:1 complex mainly originates from the dipole−dipole interaction of the CO groups of the two moieties. The interatomic distance R_{C-OC} between the C-atom of the CO group of acetone with the O-atom of acetaminophen is 3.32−3.48 Å. In this structure, the CH_3 conformation of acetaminophen is found weakly varied from the 'staggered' conformation of the monomer by a dihedral angle deviation of 8.6−15.5°. The BSSE corrected binding energy $\Delta E_{int}^{(cor)}$ ranges from −2.1 to −2.6 kcal/mol (Table 7). For all these structures, the BSSE contribution to the total interaction energy becomes gradually less significant by increasing the size of the basis set used and reaching quite comparable values at the DFT2 and DFT3 levels.

5.1.2. Predicted IR Spectra of Acetaminophen Acetone Complexes. Structure D′1 (Figure 7B). From the DFT-B3PW91 calculations, the IR band of the ν_{OH} mode of acetaminophen is strongly red-shifted by 266−294 cm^{-1}, while its intensity is enhanced by an order of magnitude (Table 8). Whereas, the IR bands associated with the NH and CO (amide 1) modes of acetaminophen are almost unaffected by the complex formation.

TABLE 5: Calculated Geometrical Parameters and Interaction Energies of the Acetaminophen-(Ethanol)$_3$ Tetramer [Eth1...HO(1) Eth2...HN(1) Eth3...OC(1)] in the Equilibrium Structure T1 Using Both HF and DFT-B3PW91 Methods[e]

	HF	DFT1	DFT2	DFT3
		structural parameters[a,b]		
$d^{(Eth1)}_{OH}$ (Å)	0.95	0.97	0.97	0.96
$d^{(Eth2)}_{OH}$ (Å)	0.95	0.97	0.97	0.96
$d^{(Eth3)}_{OH}$ (Å)	0.96 (+1.10^{-2})	0.98 (+1.10^{-2})	0.98 (+1.10^{-2})	0.97 (+1.10^{-2})
$d^{(1)}_{OH}$ (Å)	0.96 (+1.10^{-2})	0.98 (+1.10^{-2})	0.98 (+1.10^{-2})	0.97 (+1.10^{-2})
$d^{(1)}_{NH}$ (Å)	1.00 (+1.10^{-2})	1.02 (+1.10^{-2})	1.02 (+1.10^{-2})	1.02 (+1.10^{-2})
$d^{(1)}_{CO}$ (Å)	1.24 (+1.10^{-2})	1.24 (+2.10^{-2})	1.24 (+2.10^{-2})	1.23 (+1.10^{-2})
$R^{(1)}_{O\cdots HO(1)}$ (Å)	1.82	1.81	1.82	1.86
$\alpha_{O\cdots HO}$	177.0	172.3	170.5	177.9
$R^{(2)}_{O\cdots HN(1)}$ (Å)	1.99	2.00	2.03	2.04
$\alpha_{O\cdots HN}$	178.0	171.5	173.4	176.1
$R^{(3)}_{H\cdots OC(1)}$ (Å)	1.90	1.85	1.85	1.86
$\alpha_{H\cdots OC}$	118.0	113.2	115.9	117.2
		binding energy[c,d]		
$\Delta E_{int}^{(CP)}$	−22.8	−17.4	−17.2	−16.5
$\epsilon^{(2)}_{Eth...HO(1)}$	−8.8	−7.0	−6.6	−6.1
$\epsilon^{(2)}_{Eth...NH(1)}$	−7.1	−4.6	−4.4	−4.4
$\epsilon^{(2)}_{Eth...CO(1)}$	−6.8	−5.5	−5.8	−5.7
$\epsilon^{(2)}_{Eth1...Eth2}$	+0.2	+0.15	+0.1	+0.10
$\epsilon^{(2)}_{Eth1...Eth3}$	−0.1	−0.05	−0.04	−0.05
$\epsilon^{(2)}_{Eth2...Eth3}$	−0.1	−0.1	−0.1	−0.1
$\epsilon_{AEth1Eth2}^{(3)}$	+0.5	+0.4	+0.4	+0.4
$\epsilon_{AEth1Eth3}^{(3)}$	−0.2	−0.3	−0.3	−0.2
$\epsilon_{AEth2Eth3}$(3)	−0.5	−0.4	−0.5	−0.4
$\epsilon_{Eth1\ Eth2Eth3}^{(3)}$	∼0	∼0	∼0	∼0
$\epsilon^{(4)}$	∼0	∼0	∼0	∼0

[a] Abbreviations in this table: eth, ethanol solvent molecule; OH(**1**), acetaminophen hydroxyl group; NH(**1**), acetaminophen amino group; and OC(**1**), acetaminophen carbonyl group. [b] Significant bond length deviations of OH, NH, and CO functional groups from isolated acetaminophen monomer have been reported in parentheses. [c] The binding energy $\Delta E_{int}^{(cor)}$ values in this table are corrected from BSSE according to the generalized Boys-Bernardy scheme. [d] Energy unit (kcal/mol): A = acetaminophen, Eth1 = Eth...HO, Eth2 = Eth...NH, and Eth3 = Eth...CO. [e] The calculated pair interaction energy ($\epsilon^{(2)}$) as well as the 3- ($\epsilon^{(3)}$) and ($\epsilon^{(4)}$) 4-bodies interaction energy contributions corrected from the BSSE using the Site−Site Function Counterpoise method (SSFC) have been reported.[32−35]

TABLE 6: Calculated Vibrational Frequencies and IR Intensities of the OH, NH, and CO Stretching Modes and the CH Stretches of the CH$_3$ Group of Acetaminophen and the ν_{OH} Stretching Mode of the Ethanol Species in the Equilibrium Structure T1 Using the DFT-B3PW91 Procedure (See Text)[d]

	DFT1			DFT2		
	freq (cm^{-1})	$\Delta\nu$ (cm^{-1})	I_{IR} (km/mol)	freq (cm^{-1})	$\Delta\nu$ (cm^{-1})	I_{IR} (km/mol)
$\nu^{(1)}$(OC)	1754.3	−49.0	438.9	1735.5	−40.8	473.7
ν_s(CH)	3079.6	+7.6	6.1	3073.4	+4.1	6.8
ν_a(CH)	3154.9	−0.5	10.0	3149.6	−1.8	2.7
	3186.5	+27.5	2.4	3166.2	+10.5	11.8
$\nu^{(1)}$(NH)	3527.7	−112.3	637.4	3516.8	−119.8	303.6
$\nu^{(1)}$(OH)	3530.7	−260.4	997.4	3522.4	−265.9	1360.1
$^a\nu^{(eth)}_{OH}$	3561.1	−233.1	611.4	3550.1	−245.9	758.7
$^b\nu^{(eth)}_{OH}$	3803.9	+9.7	34.6	3790.9	−5.1	39.7
$^c\nu^{(eth)}_{OH}$	3812.0	+17.8	34.0	3793.4	−2.6	37.0
low freq (cm^{-1})	11.0 13.7 27.7 37.2 70.1 80.6	16.0 19.5 38.3 50.0 88.5 94.1	22.1 25.6 58.7 66.8 105.2 126.8	6.8 11.1 22.9 28.6 61.8 70.4	12.6 15.4 33.8 45.3 76.4 89.6	18.2 12.5 50.7 54.3 94.3 114.0

[a] HBD EthO(H,D)...CO(**1**). [b] HBA EthO(H,D)...OH(**1**). [c] HBA EthO(H,D)...NH(**1**). [d] The calculated low frequency values arising under the complex formation have been also reported.

The IR bands associated respectively with the ν_{OH} and ν_{NH} stretching modes of acetaminophen are well-separated, the less intense ν_{NH} band being situated at a lower frequency than the intense ν_{OH} line (Figure 7B). The IR bands of the ν_{CO} modes of the two moieties form a doublet structure separated by a few wavenumbers for which the intensity ratio varies significantly according to the basis sets used (Table 8). For HBA acetone, the ν_{CO} mode is found to be red-shifted under the complex formation by 26−33 cm^{-1}. In contrast, the band center position of the IR band of the ν_{CCC} stretching mode is shifted toward higher wavenumbers by 17−30 cm^{-1}, while its integrated intensity is significantly decreased.

Structure D′2 (Figure 8A). The main spectral signature of the 1:1 complex (structure D′2) is perceived on the ν_{NH} mode of acetaminophen which is found red-shifted by 110−127 cm^{-1}, while its intensity is enhanced by an order of magnitude (Table 8). Even if, the frequency shift of this mode is found less significant than for acetaminophen interacting with ethanol (structure D2), the predicted intensity changes are found quite similar under the complex formation. As expected, the intensity and frequency band center position of the ν_{OH} mode of acetaminophen are almost unaffected. The ν_{CO} mode of acetaminophen is modestly red-shifted by 6.5−9.0 cm^{-1}, and its intensity increases by 20−40%.

For HBA acetone, the ν_{CO} mode is red-shifted by 21−46 cm^{-1} with an intensity enhancement of 20−40%. As a consequence, the two ν_{CO} bands of the moieties display a well-defined doublet structure separated by 12−26 cm^{-1}; the band situated

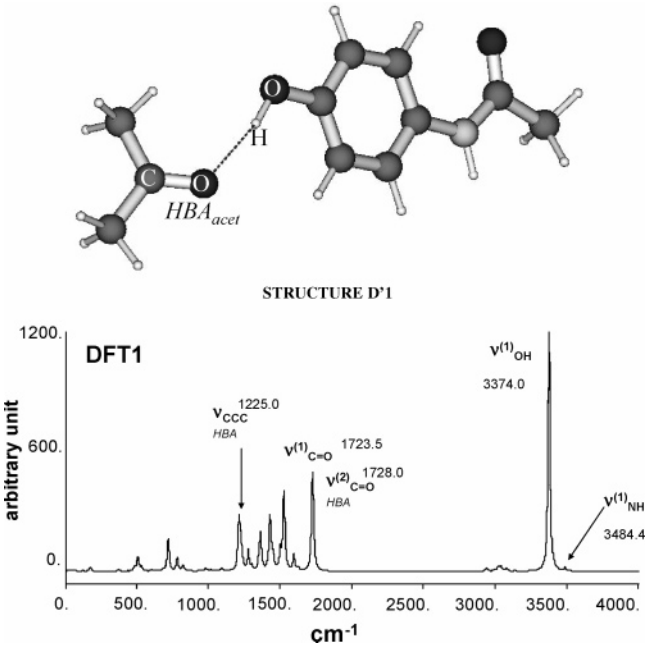

Figure 7. Calculated IR spectrum (scaled frequencies) of the 1:1 acetaminophen complex formed with acetone in the equilibrium structure D′1 at the DFT1 level.

at lower wavenumbers is assigned to the ν_{CO} mode of acetaminophen. Under the complex formation, the ν_{CCC} mode is shifted toward higher wavenumbers but only by a few wavenumbers.

Structure D′3 (Figure 8B). In dimer structure D′3, the IR lines of the ν_{OH} and ν_{NH} stretches of acetaminophen are weakly affected under the complex formation (Table 8). The main spectral features are perceived on the ν_{CO} modes of the two moieties which are red-shifted by 15−24 cm^{-1} especially for the ν_{CO} stretching mode of acetaminophen (Table 8). Thus, they form a well-defined doublet in which the mode situated at the lowest frequency is again assigned to the CO mode of acetaminophen. Under the complex formation, their intensities are respectively increased and decreased by 10% for acetone and acetaminophen. Under the complex formation, the ν_{CCC} mode is shifted toward higher wavenumbers by 25.5−30.0 cm^{-1}, while its intensity is decreased.

The frequency shifts and intensity changes of the ν_s(CH) and ν_a(CH) modes of the CH_3 group of acetaminophen in dimer structures D′1, D′2, and D′3 present similar spectral features to those obtained for the 1:1 complexes formed with ethanol. In structure D′1, the IR intensity of these modes remains as expected, close to that of isolated acetaminophen (Table 8). The most intense band of the ν_a(CH) doublet structure corresponds with the lowest vibrational frequency, and their spectral separation is weakly perturbed by interactions with acetone.

The most significant frequency shifts and intensity changes of the ν_s(CH) and ν_a(CH) modes are however found for acetone interacting with the NH group of acetaminophen (structure D′2). Indeed, the most intense band of the ν_a(CH) doublet structure is now situated at the highest frequency (as for interaction with ethanol). In structure D′3, the most intense ν_a(CH) band of the doublet structure again corresponds to the IR line situated at the lowest vibrational frequency. The spectral separation between the IR lines of the ν_a(CH) modes increases due to the CH_3 conformational deviation under the complex formation compared with the 'eclipsed' one for the acetaminophen monomer.

5.2. Acetaminophen (Acetone)$_3$ Complex. *5.2.1. Structure and Binding Energy.* We have determined the equilibrium structure of the 1:3 complex (Figure 9) in which one acetone molecule interacts with each of the three CO, OH, and NH groups of acetaminophen (structure T′1). The calculated structural parameters are gathered in Table 9 with the irreducible 2-, 3-, and 4-bodies contributions to the total interaction energy. The calculated $R^{(1)}{}_O\cdots HO$ (i.e. between the O-atom of acetone and the proton of the OH group) and $R^{(2)}{}_O\cdots HN$ (i.e. between the O-atom of acetone and the proton of the NH group) distances are 1.84 Å and 2.01−2.06 Å, respectively, whereas the interatomic $R^{(3)}{}_C\cdots OC$ distance is found varying from 3.37 to 3.61 Å (Table 9). In marked contrast to the complex formed with ethanol species (structure T1), the structural arrangement of the acetone molecules with acetaminophen does not appear like a quasi superposition of each individual dimer structure. In particular, the calculated relative angles in the tetramer are found to significantly deviate from their calculated values in each corresponding individual dimer structure (cf. Table 7).

In the tetramer, the pair interaction energy between acetaminophen and HBA acetone interacting with the OH group is close to the calculated value in the dimer structure D′1 because such a structural arrangement is almost unperturbed by the presence of the two other farthest acetone molecules. In contrast, the pair interaction energies involving an acetone molecule interacting with either the NH group (hydrogen-bond) or the CO group (dipole−dipole) of acetaminophen are found slightly less stabilizing (in particular for the pair interaction involving the amino group) in comparison with the pair energy values reported in dimer structures D′2 and D′3. This is due to the competition taking place between the dipole−dipole interactions between the acetone molecules and the acetone-acetaminophen. We emphasize that such significant deviations of these pair interaction energies compared with the calculated interaction energies in dimer structures D′2 and D3 are mainly due to the attractive irreducible 3-bodies contributions (~ -1.0 kcal/mol) to the stabilization energy (cf. Table 9). Despite such cooperative effects, we notice that the irreducible 4-bodies contribution remains nevertheless negligible in the stabilization of the 1:3 complex.

5.2.2. Predicted IR Spectrum (Figure 9B). The main IR spectral signatures have been reported in Table 10. As for the 1:1 complexes, the hydrogen-bonded interactions involved in the stabilization of the equilibrium tetramer T′1 are perceived on the frequency red-shifts and the intensity enhancements of the ν_{OH} and ν_{NH} modes of acetaminophen (Table 10). Under the complex formation, the ν_{OH} mode of acetaminophen is red-shifted by 250−260 cm^{-1} with an IR intensity enhanced by an order of magnitude, whereas the ν_{NH} mode is shifted toward lower wavenumbers by 120−145 cm^{-1} and its IR intensity modestly decreased by 6−12%. The spectral separation between these two bands (the ν_{NH} mode being situated at a lowest frequency) varies from 25 to 35 cm^{-1}.

For acetone species, the main spectral signatures are perceived on the well-defined triplet structure formed by their ν_{CO} stretching modes which have been shifted toward lower wavenumbers by 21−36 cm^{-1} under complex formation. This frequency shift is accompanied by a significant intensity enhancement (Table 10). It is noteworthy that the ν_{CO} modes of acetone species (especially interacting with its NH and CO groups) cannot be legitimately disentangled from the ν_{CO} mode of acetaminophen. Indeed, they are strongly coupled together primarily due to the acetone-acetaminophen interactions and indirectly with the δ_{CNH} and δ_{OCN} modes of acetaminophen which are also coupled with the ν_{CO} mode of acetaminophen

TABLE 7: Calculated Geometrical Parameters and Interaction Energies in Global and Local Energy Minimum Structures of the Acetaminophen-Acetone Dimer Using Both HF and DFT-B3PW91 Methods[a]

structural parameters[b] and binding energies[c,d]

	structure D′1 [Acet...HO(**1**)]				structure D′2 [Acet...NH(**1**)]				structure D′3 [Acet...CO(**1**)]			
a	HF	DFT1	DFT2	DFT3	HF	DFT1	DFT2	DFT3	HF	DFT1	DFT2	DFT3
$d^{(2)}_{CO}$ (Å)	1.22	1.22 ($+1.10^{-2}$)	1.22 ($+1.10^{-2}$)	1.22 ($+1.10^{-2}$)	1.22	1.22	1.22 ($+1.10^{-2}$)	1.21	1.22	1.22 ($+1.10^{-2}$)	1.22 ($+1.10^{-2}$)	1.21
$d^{(1)}_{OH}$ (Å)	0.96 ($+1.10^{-2}$)	0.98 ($+2.10^{-2}$)	0.98 ($+1.10^{-2}$)	0.98 ($+2.10^{-2}$)	0.95	0.97	0.97	0.96	0.95	0.97	0.97	0.96
$d^{(1)}_{NH}$ (Å)	0.99	1.01	1.01	1.01	1.00 ($+5.10^{-3}$)	1.02 ($+1.10^{-2}$)	1.02 ($+1.10^{-2}$)	1.02 ($+1.10^{-2}$)	0.99	1.01	1.01	1.01
$d^{(1)}_{CO}$ (Å)	1.23	1.22	1.22	1.22	1.23	1.22	1.22	1.22	1.24 ($+1.10^{-2}$)	1.23 ($+1.10^{-2}$)	1.23 ($+1.10^{-2}$)	1.22 ($+1.10^{-2}$)
$R_{O\cdots HO}$ (Å)	1.88	1.83	1.83	1.83								
$\alpha_{O\cdots HO(1)}$	166.2	167.3	170.0	169.1								
$R_{O\cdots HN}$ (Å)					2.07	2.04	2.07	2.07				
$\alpha_{O\cdots HN(1)}$					179.4	170.7	171.5	170.6				
$R_{C\cdots OC}$ (Å)									3.16	3.32	3.48	3.45
$\alpha_{C\cdots OC(2)}$									98.1	100.7	100.3	98.6
$\Delta E_{int}^{(cor)}$	−8.1	−6.8	−7.0	−7.0	−6.8	−4.5	−4.7	−4.8	−4.8	−2.1	−2.3	−2.6
$\Delta E_{int}^{(BSSE)}$	+3.7	+2.3	+0.4	+0.1	+3.6	+2.1	+0.3	+0.3	+3.7	+0.5	+0.3	+0.2
$\Delta E_{int}^{(ZPE)}$	+1.3	+1.3	+1.2	+1.2	+1.0	+0.9	+0.8	+0.9	+1.0	+0.9	+0.6	+0.7

[a] BSSE and ZPE contributions to the binding energy have been also reported in this table for each of the dimer structures investigated. HF = HF/6-31G DFT1 = B3PW91/6-31G*, DFT2 = B3PW91/6-31+G*, DFT3 = B3PW91/6-311++G**. Abbreviations in this table: acet = acetone solvent molecule; OH(**1**), acetaminophen hydroxyl group; NH(**1**), acetaminophen amino group; and OC(**1**), acetaminophen carbonyl group. [b] Significant bond length deviations of OH, NH, and CO functional groups from isolated acetaminophen monomer have been reported in parentheses. [c] The binding energy $\Delta E_{int}^{(cor)}$ values in this table are corrected from BSSE according to the generalized Boys-Bernardy scheme. [d] Energy unit (kcal/mol).

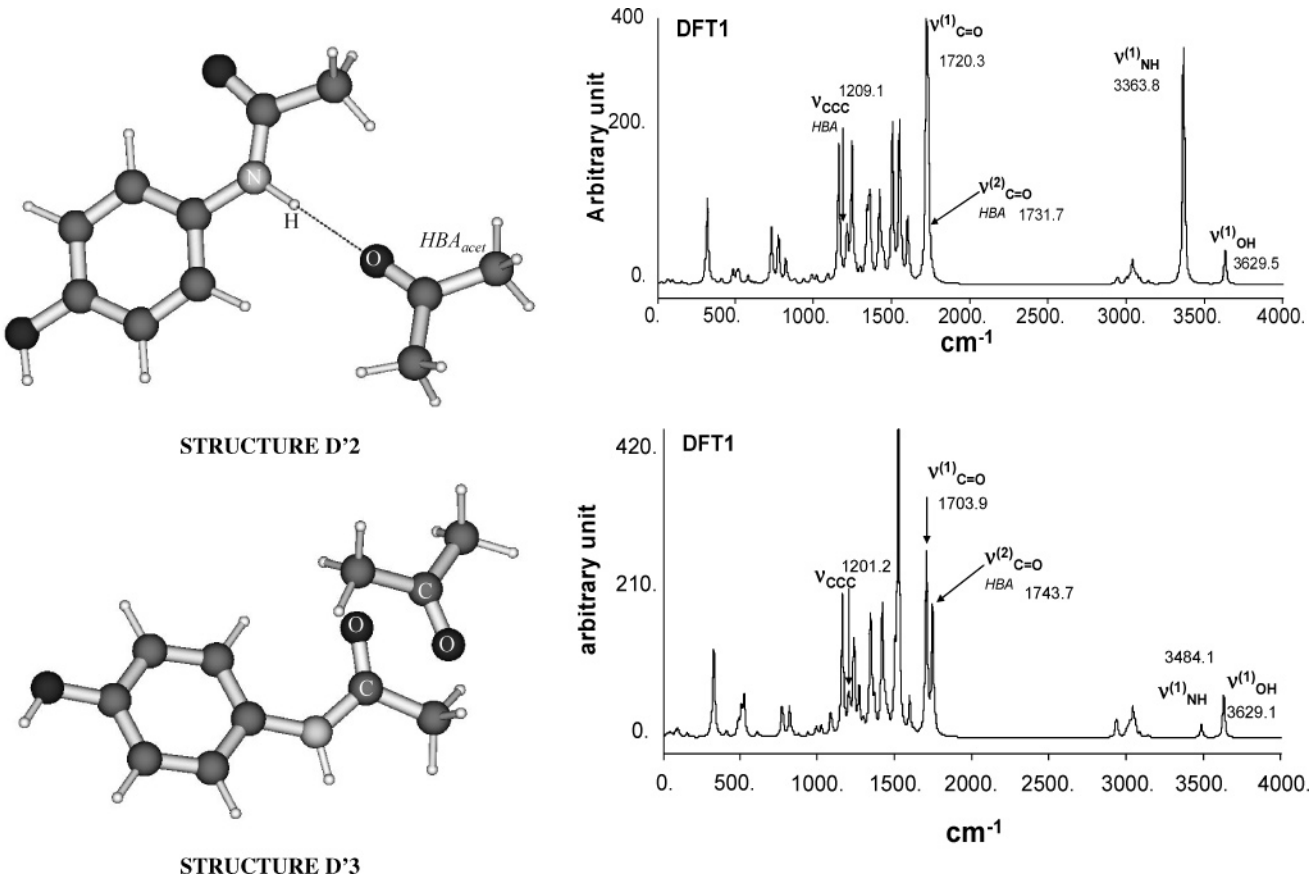

Figure 8. Calculated IR spectrum (scaled frequencies) of the 1:1 acetaminophen complex formed with acetone in structures D′2 and D′3 (local energy minima) at the DFT1 level.

itself. However, it was possible from further vibrational analysis to distinguish in the triplet structure the IR line of the ν_{CO} mode of acetone interacting with the OH group of acetaminophen although weak couplings with other internal motions of the carbon skeleton of the phenol ring exist (Figure 9). The IR band of this ν_{CO} mode of acetaminophen is situated at the lowest frequency and has the lowest intensity even found enhanced under the complex formation. The IR lines of the ν_{CCC} modes of acetone also exhibit a well-defined triplet structure in which the two vibrational transitions situated at higher frequencies have more significant intensity enhancements than those found in dimer structures (cf. calculated values in Tables 8 and 10). The most intense band of the ν_{CCC} triplet structure is situated at an intermediate frequency.

TABLE 8: Vibrational Analysis of Acetaminophen-Acetone 1:1 Complexes in Structures D′1, D′2, and D′3 from the DFT-B3PW91 Procedure: Calculated Vibration Frequencies and IR Intensities Associated with the OH, NH, and CO Internal Modes and the CH Stretches of the CH_3 Group of Acetaminophen and the Antisymmetric ν_{CCC} and Symmetric ν_{CO} Stretching Modes for Acetone

structure D′1

	DFT1		DFT2		DFT3	
low freq (cm^{-1})	14.3 24.2 27.9 41.4 52.5 66.7		8.1 21.7 22.6 43.0 54.9 62.8		7.6 18.9 22.1 40.6 48.5 61.0	
internal modes	ν (cm^{-1})	I_{IR} (km/mol)	ν (cm^{-1})	I_{IR} (km/mol)	ν (cm^{-1})	I_{IR} (km/mol)
$\nu^{(1)}_{OC}$	1800.3 (−3.4)	304.6	1771.6 (−4.7)	320.5	1762.7 (−4.7)	329.5
ν_s(CH)	3070.5 (−1.5)	11.8	3061.3 (−8.0)	5.7	3050.3 (−1.1)	11.9
ν_a(CH)	3153.4 (−2.0)	17.8	3128.3 (−23.1)	7.5	3132.2 (−0.5)	16.7
	3157.8 (−1.2)	5.5	3182.7 (+27.2)	5.8	3134.1 (−0.8)	4.3
$\nu^{(1)}_{NH}$	3639.9 (−0.2)	15.4	3636.4 (−0.2)	16.4	3647.9 (+0.4)	20.4
$\nu^{(1)}_{OH}$	3524.5 (−266.6)	1176.8	3529.2 (−259.1)	1330.4	3573.5 (−294.0)	1377.6
$\nu_a{}^{(2)}_{CCC}$	1279.6 (+29.9)	139.8	1276.6 (+27.5)	222.0	1262.3 (+25.6)	186.1
$\nu^{(2)}_{CO}$	1805.1 (−33.9)	229.0	1790.3 (−23.9)	316.8	1779.3 (−26.0)	328.6

structure D′2

	DFT1		DFT2		DFT3	
low freq (cm^{-1})	13.9 20.9 29.6 45.2 47.4 62.3		10.3 14.0 23.0 40.9 61.2 64.8		10.8 13.1 23.1 40.8 60.5 63.2	
internal modes	ν (cm^{-1})	I_{IR} (km/mol)	ν (cm^{-1})	I_{IR} (km/mol)	ν (cm^{-1})	I_{IR} (km/mol)
$\nu^{(1)}_{OC}$	1797.1 (−6.6)	326.6	1768.3 (−8.0)	342.9	1758.9 (−8.5)	360.9
ν_s(CH)	3064.9 (−7.1)	3.9	3071.3 (+2.0)	5.8	3052.8 (+1.4)	9.0
ν_a(CH)	3125.5 (−29.9)	0.7	3148.5 (−2.9)	5.1	3128.7 (−5.0)	5.6
	3131.9 (−27.1)	8.0	3161.6 (+6.1)	13.8	3143.3 (+8.4)	11.5
$\nu^{(1)}_{NH}$	3513.9 (−126.6)	345.4	3526.2 (−110.4)	328.9	3526.7 (−120.8)	339.6
$\nu^{(1)}_{OH}$	3791.3 (+0.2)	50.5	3788.9 (+0.6)	57.8	3868.7 (+1.2)	71.4
$\nu_a{}^{(2)}_{CCC}$	1263.4 (+13.7)	46.7	1248.4 (−1.0)	41.5	1248.4 (+11.7)	55.7
$\nu^{(2)}_{CO}$	1809.0 (−30.0)	193.1	1794.3 (−45.9)	250.6	1783.9 (−21.4)	257.5

structure D′3

	DFT1		DFT2		DFT3	
low freq (cm^{-1})	8.3 24.1 33.2 43.9 53.3 64.0		7.3 22.2 23.4 38.8 45.2 56.6		6.5 14.5 24.5 32.9 50.4 57.6	
internal modes	ν (cm^{-1})	I_{IR} (km/mol)	ν (cm^{-1})	I_{IR} (km/mol)	ν (cm^{-1})	I_{IR} (km/mol)
$\nu^{(1)}_{OC}$	1779.9 (−23.8)	253.6	1762.1 (−14.2)	257.6	1751.9 (−15.5)	253.0
ν_s(CH)	3068.0 (−4.0)	15.5	3066.5 (−2.8)	15.4	3046.4 (−5.0)	15.5
ν_a(CH)	3152.5 (−2.9)	7.1	3148.5 (−2.9)	8.3	3126.0 (−7.7)	6.3
	3158.7 (−0.8)	11.6	3156.7 (+1.2)	15.4	3139.2 (+4.3)	10.8
$\nu^{(1)}_{NH}$	3639.5 (−0.5)	19.1	3636.1 (−0.5)	19.3	3645.3 (−2.2)	23.4
$\nu^{(1)}_{OH}$	3791.0 (−0.1)	59.4	3788.1 (−0.2)	66.5	3868.2 (+0.7)	81.3
$\nu_a{}^{(2)}_{CCC}$	1254.8 (+5.1)	45.6	1240.0 (+4.2)	40.6	1240.0 (+3.3)	35.6
$\nu^{(2)}_{CO}$	1821.5 (−17.5)	253.6	1800.8 (−13.4)	257.6	1790.6 (−14.7)	231.3

6. Discussion and Conclusion

The predicted structures and IR spectral features presented so far concerning acetaminophen complexes with ethanol or acetone molecules can now be critically discussed from a comparison with IR measurements reported in the literature.[1] One of the issues will concern the influence of the exchange contribution on the vibrational spectroscopic features of such complexes taken into account using the DFT-B3PW91 method (versus the HF calculations). However, we can preliminarily emphasize that similar equilibrium and local energy minimum structures of the acetaminophen 1:1 and 1:3 complexes (formed with either ethanol or acetone) have been predicted using the HF and the DFT-B3PW91 methods.

As far as we know, there are no experimental data available in the literature concerning directly the structural determination of acetaminophen complexes formed with either ethanol or acetone species (complex structures and binding energies). Nevertheless, as we will see below, theoretical chemistry calculations can provide first physical insights about the specific interactions governing the solvation mechanism around acetaminophen in ethanol and acetone solvents as combined with a further analysis of the spectral features observed by IR absorption spectroscopy.

6.1. Structural Properties. To summarize, the 1:1 complexes of acetaminophen formed with alcohol are mainly stabilized through intermolecular hydrogen-bonded interactions between the chemical OH, NH, and CO functional groups of acetaminophen and the O atom of HBA ethanol or proton of the hydroxyl proton of HBD ethanol. In other terms, the OH and NH groups of acetaminophen act as proton donor centers, whereas the CO group plays the role of proton acceptor center. As expected, the predicted total binding energies are found less stabilizing by including the exchange-correlation contribution (in the DFT calculations) even if the structural arrangements (interatomic distances and relative orientations) in the dimer structures are found quite comparable from both HF and DFT-B3PW91 calculations. Nevertheless, the pair interaction energy associated with HBA ethanol interacting with the OH group of acetaminophen is always found at lower values (more stabilizing) than those involving ethanol with the NH and CO functional groups. For the hydrogen-bonded 1:3 complex of acetaminophen formed with ethanol, the equilibrium structure appears as a superposition of the three dimer structures (D1, D2, and D3). The stabilization of this tetramer mainly results from the pair interaction energy contributions involving acetaminophen, whereas the ethanol−ethanol pair interaction energies are nearly negligible. Moreover, the irreducible 3-bodies interaction contributions to the total interaction energy are found rather small as well as the irreducible 4-bodies interaction component can be quite neglected here.

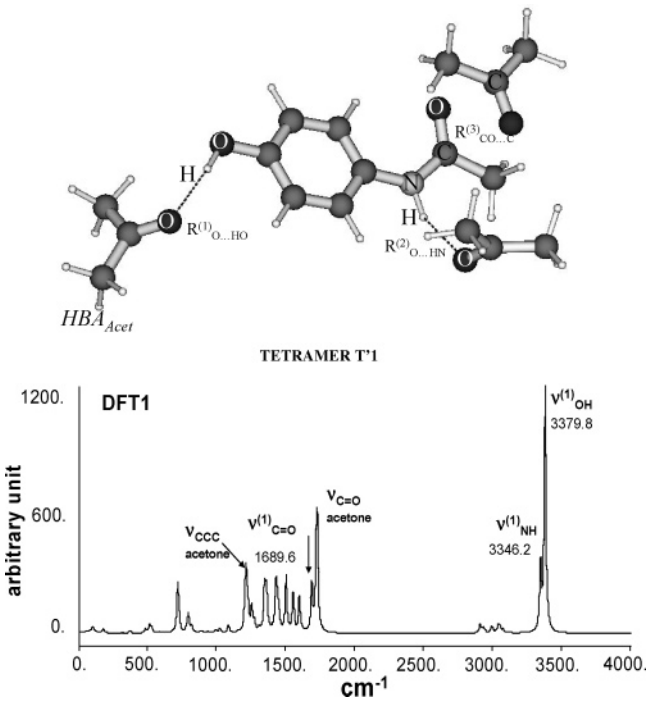

Figure 9. Calculated IR spectrum (scaled frequencies) of the 1:3 acetaminophen complex formed with acetone in structure T′1 at the DFT1 level.

The stabilization of the complexes of acetaminophen formed with acetone involves both intermolecular hydrogen-bond and dipole−dipole interactions. Again, the chemical OH and NH functional groups of acetaminophen play the role of proton donor centers. The pair interaction energies involving these functional groups with HBA acetone are less stabilizing than their corresponding pair energy values with HBA ethanol. Due to the charge distribution on the CO groups, acetaminophen mainly interacts with acetone through electrostatic dipole−dipole interactions. Consequently, the total binding energies for complexes of acetaminophen formed with acetone are found less stabilizing than those formed with ethanol (using the HF method as well as the DFT-B3PW91 procedure). Nevertheless, the structural arrangements, i.e., interatomic distances and relative orientations between acetone and acetaminophen, and the calculated binding energies are slightly modified by including the exchange contribution though the B3PW91 function (DFT calculations). As for acetaminophen interacting with ethanol, the pair interaction energy between HBA acetone and the OH group of acetaminophen is found to be the most stabilizing compared with those involving interactions of acetone with the NH and CO functional groups. The intermediate contribution to binding energy is however due to the intermolecular hydrogen bonding between acetone and the NH group of acetaminophen with a value quite comparable to the pair interaction energy involved in HBA ethanol. The lowest pair interaction energy contribution to the binding energy originates from the dipole−dipole interactions between acetone and the CO group of acetaminophen. Finally, the equilibrium structure of the 1:3 complex of acetaminophen formed with acetone does not result from a superposition of the dimer structures (D′1, D′2, and D′3) because of a subtle balance taking place between the dipole−dipole interactions originating from the pair of the acetone molecules interacting with the NH and CO groups of acetaminophen and the intermolecular interaction involving the CO groups of the acetone and acetaminophen moieties. This interpretation about the existence of a competitive mechanism

TABLE 9: Calculated Geometrical Parameters and Interaction Energies of the Acetaminophen-(Acetone)$_3$ Tetramer [Acet1...HO(1) Acet2...HN(1) Acet3...OC(1)] in the Equilibrium Structure T′1 Using Both HF and DFT-B3PW91 Methods[d]

	HF	DFT1	DFT2
structural parameters[a]			
$d^{(Acet1)}_{CO}$ (Å)	1.22	1.22 (+1.10^{-2})	1.22 (+1.10^{-2})
$d^{(Acet2)}_{CO}$ (Å)	1.23 (+1.10^{-2})	1.22 (+1.10^{-2})	1.22 (+1.10^{-2})
$d^{(Acet3)}_{CO}$ (Å)	1.22	1.22 (+1.10^{-2})	1.22 (+1.10^{-2})
$d^{(1)}_{OH}$ (Å)	0.96 (+1.10^{-2})	0.98 (+1.10^{-2})	0.98 (+1.10^{-2})
$d^{(1)}_{NH}$ (Å)	1.00 (+5.10^{-3})	1.02 (+1.10^{-2})	1.02 (+1.10^{-2})
$d^{(1)}_{CO}$ (Å)	1.24 (+1.10^{-2})	1.23 (+1.10^{-2})	1.23 (+1.10^{-2})
$R^{(1)}_{O\cdots HO(1)}$ (Å)	1.89	1.84	1.84
$\alpha_{O\cdots HO}$	164.9	167.0	169.4
$R^{(2)}_{O\cdots HN(1)}$ (Å)	2.10	2.01	2.06
$\alpha_{O\cdots HN}$	147.0	161.7	160.2
$R^{(3)}_{C\cdots OC}$ (Å)	3.30	3.37	3.61
$\alpha_{C\cdots OC}$	89.9	89.0	88.3
binding energy[b,c]			
$\Delta E_{int}^{(CP)}$	−21.5	−14.8	−15.1
$\epsilon(2)_{Acet...HO(1)}$	−8.0	−6.8	−7.0
$\epsilon^{(2)}_{Acet...NH(1)}$	−5.2	−4.1	−4.2
$\epsilon(2)_{Acet...CO(1)}$	−4.4	−2.0	−2.1
$\epsilon(2)_{Acet1...Acet2}$	∼0	∼0	+0.1
$\epsilon(2)_{Acet1...Acet3}$	∼0	∼0	∼0
$\epsilon(2)_{Acet2...Acet3}$	−2.7	−1.0	−1.1
$\epsilon_{AAcet1Acet2}(3)$	+0.3	+0.3	+0.3
$\epsilon_{AAcet1Acet3}(3)$	−0.1	−0.1	−0.1
$\epsilon_{AAcet2Acet3}(3)$	−1.4	−1.1	−1.0
$\epsilon_{Acet1\ Acet2Acet3}(3)$	∼0	∼0.	∼0
$\epsilon^{(4)}$	∼0	∼0.	∼0

[a] Significant bond length deviations of OH, NH, and CO functional groups from isolated acetaminophen monomer have been reported in parentheses. [b] The binding energy $\Delta E_{int}^{(cor)}$ values in this table are corrected from BSSE according to the generalized Boys-Bernardy scheme. [c] Energy unit (kcal/mol): A = acetaminophen, Acet1 = Acet...HO, Acet2 = Acet...NH, and Acet3 = Acet...CO. [d] See also legend of Table 5 for details. Abbreviations in this table: acet, acetone solvent molecule; OH(**1**), acetaminophen hydroxyl group; NH(**1**), acetaminophen amino group; OC(**1**), acetaminophen carbonyl group.

is reinforced by the fact that nonadditive contributions to the interaction energy significantly arise from the irreducible 3-bodies interactions between a pair of acetone interacting with the NH and CO groups of acetaminophen. The attractive energy contribution resulting from the 3-bodies interaction processes (∼ −1. kcal/mol) adds favorably to the pair interaction energy contributions in a cooperative effect to stabilize the tetramer structure. From these structural findings, we conclude that the stabilization of the complexes of acetaminophen formed with ethanol is greater than with acetone. With ethanol, the binding energy is strengthened because the CO group of acetaminophen interacts through an intermolecular hydrogen-bonding with the proton of ethanol, whereas with acetone, electrostatic (dipole−dipole) interactions are only involved even if an additional contribution due to attractive 3-bodies interactions takes place.

6.2. Vibrational Signatures of Acetaminophen Complexes. *6.2.1. Acetaminophen Moiety.* The hydrogen-bond nature of the intermolecular solute−solute interactions are perceived on the spectral signatures of the ν_{OH} and ν_{NH} stretching modes of acetaminophen interacting with the O-atom of either HBA ethanol or HBA acetone. These spectral signatures are characterized by significant frequency shifts toward lower wavenumbers and intensity enhancements of an order of magnitude. With HBA ethanol, the frequency red-shifts of the ν_{OH} and ν_{NH} modes are typically 260−265 cm^{-1} and 110−120 cm^{-1}, respectively. With acetone, the frequency red-shifts are less significant with values of about 250 cm^{-1} and 120−145 cm^{-1}. Including the exchange-correlation component in the DFT-B3PW91 calcula-

TABLE 10: Calculated Vibrational Frequencies and IR Intensities of the OH, NH, and CO Stretching Modes and the CH Stretches of the CH_3 Group of Acetaminophen and the Antisymmetric ν_a(CCC) and Symmetric ν_{CO} Stretching Modes for Acetone Species in the Equilibrium Structure T′1 from the DFT-B3PW91 Procedure (See Text)[a]

	DFT1			DFT2		
	freq (cm^{-1})	$\Delta\nu$ (cm^{-1})	I_{IR} (km/mol)	freq (cm^{-1})	$\Delta\nu$ (cm^{-1})	I_{IR} (km/mol)
$\nu^{(1)}$(OC)	1765.0	−38.0	222.1	1748.6	−30.7	248.3
ν_s(CH)	3074.2	+2.2	7.0	3072.1	+2.8	9.5
ν_a(CH)	3153.8	−1.6	3.4	3148.6	−2.8	5.3
	3173.1	+14.1	6.0	3167.3	+11.8	9.5
$\nu^{(1)}$(NH)	3495.5	−144.5	310.7	3514.4	−122.2	261.5
$\nu^{(1)}$(OH)	3530.6	−260.5	1166.5	3538.6	−249.7	1277.6
	1259.3	+9.7	31.8	1256.6	+7.2	45.2
ν_a(CCC)	1264.1	+14.4	158.9	1257.2	+7.8	203.2
	1266.3	+16.6	96.5	1263.7	+14.3	65.0
$\nu^{(acet)}_{CO}$	1799.4	−39.6	238.1	1784.5	−29.7	227.9
$\nu^{(acet)}_{CO}$	1805.0	−34.0	245.0	1790.4	−23.8	302.7
$\nu^{(acet)}_{CO}$	1809.2	−29.8	250.2	1793.1	−21.1	284.3
low	11.6 14.4	20.6 21.3	26.7 31.9	6.4 11.3	15.1 18.5	21.2 24.4
freq	40.7 47.7	53.4 57.0	65.4 67.6	29.0 34.9	37.1 42.0	45.8 59.2
(cm^{-1})	75.9 78.2	86.2 93.1	93.7 104.5	62.8 64.3	69.6 73.1	75.0 84.3

[a] The calculated low frequency values arising from the complex formation have been also reported.

tions, the predicted ν_{NH} and ν_{OH} IR bands of acetaminophen interacting with ethanol as well as acetone are found separated by only a few wavenumbers, even if this spectral separation is found slightly more pronounced with acetone.

6.2.2. Solvent Moiety. The hydrogen-bonded character of the intermolecular interaction is also perceived on the spectral changes under the complex formation of the $\nu^{(eth)}_{OH}$ mode of HBD ethanol which is significantly red-shifted by about 230−250 cm^{-1} and accompanied by an IR intensity enhancement of an order of magnitude. We emphasize that the exchange-correlation component included in the DFT calculations appears as a substantial contribution to the frequency shift of this mode as ethanol acts as the hydrogen-bond donor center. In contrast, the frequency shift and intensity change of the ν_{OH} mode of HBA ethanol are more modestly perturbed by interactions with acetaminophen.

For acetone complexes with acetaminophen, the main spectral signature related is mainly observed on the ν_{CO} mode which is red-shifted by about 25−40 cm^{-1} with a significantly enhanced intensity.

Nevertheless, we surmise that it is only via IR measurements of acetaminophen diluted in liquid or supercritical (solvent) ethanol and acetone that it will be possible to make a distinction between the DFT or HF predictions.

6.3. Comparison with IR Measurements. We have recently investigated the solvation phenomenon of acetaminophen in CO_2-expanded organic solvents, namely ethanol and acetone (acetaminophen diluted in liquid or supercritical (solvent) mixture) using absorption spectrometry in the mid-infrared (MIR) domain.[1] Due to the existence of the hydrogen-bond network between ethanol in the CO_2-expanded ethanol, the IR spectrum associated with the ν_{OH} stretching mode of ethanol presents a very broad and intense band due to the overlapping of the ν_{NH} and ν_{OH} transitions of acetaminophen. To measure the IR spectra of acetaminophen in CO_2-expanded ethanol in the region of the ν_{NH} and ν_{OH} stretching modes (3100−3600 cm^{-1}), we used deuterated ethanol (C_2H_5OD). Under such conditions, the proton of the OH group of the phenol ring of acetaminophen is substituted by deuterium. As a consequence, it is only the asymmetric IR profile of the ν_{NH} mode which subsists in this region, an assignment supported by H NMR spectroscopic measurements.[43] The evolution with the CO_2 concentration of the ν_{NH} profile has been investigated in conjunction with that of the ν_{CO} mode of acetaminophen situated in the spectral range 1650−1700 cm^{-1}. Again, the IR profiles of the ν_{NH} and ν_{OH} stretching modes of acetaminophen are found overlapping in the CO_2-expanded acetone mixture. To separate properly these two contributions in the composite profile, we have compared the IR spectra of acetaminophen in CO_2-expanded acetone with those measured for 4-(ethoxyphenyl)-acetamide under the same conditions. In the latter solute, the hydroxyl group of acetaminophen is replaced by an ethoxyl group, and only the NH functional group is present. From this comparison, it was then possible to assign the ν_{NH} stretch of acetaminophen in CO_2-expanded acetone as the spectral component observed at lower frequency. The IR measurements analysis was allowed to quantify the solvent-induced frequency shifts of the ν_{CO} and ν_{NH} modes of acetaminophen in CO_2-expanded ethanol as 30 and 150 cm^{-1}, respectively, and 20 and 100 cm^{-1} in CO_2-expanded acetone. These values can be compared with the calculated frequency shifts, in particular for the tetramer of structures T1 and T′1, respectively, which are likely the most representative spectral features related to the solvation mechanism taking place in the real solutions (Tables 6 and 10). From this comparison, a qualitative good agreement was achieved between the IR measurements in CO_2-expanded ethanol and acetone (liquid and SC fluid mixtures) and the predicted spectral features obtained from both HF and DFT calculations. However, the calculated frequency shifts using the DFT procedure appears in slightly quantitative better agreement particularly for the ν_{CO} mode of acetaminophen and the ν_{OH} mode of HBD ethanol. Therefore, we come to the conclusion that the exchange-correlation contribution is likely needed for determining the IR spectral features of the hydrogen-bonded complexes of acetaminophen formed with ethanol as well as for acetaminophen complexes formed with acetone. Indeed, the nonlocal correlation considered through the B3PW91 functional differently treats the charge distribution variations on the CO, NH, and CH_3 chemical functions of acetaminophen compared with HF calculations. This effect is also responsible for the predicted non-negligible rotational barrier of the CH_3 group of acetaminophen. Nevertheless, it comes out that matrix isolation IR experiments as well as high-resolution IR spectroscopy and Molecular Beam Electric Resonance (MBER) measurements in the gaseous phase could be needed to validate the theoretical predictions (structure and IR spectra) discussed in this paper.

To conclude, quantum chemistry calculations can provide useful first insights for understanding elaborate mechanisms such

as the preferential solvation of acetaminophen in CO_2-expanded organic solvents from the knowledge of the acetaminophen-solvent interactions. Their specificity or nonspecificity is revealed by interaction-induced perturbations on the vibrational probes (microscopic observables) leading to spectral signatures attesting the presence of transient hydrogen-bonded acetaminophen complexes formed with ethanol and acetone. We conclude that the solute−solvent interactions are slightly stronger with ethanol than with acetone, even if hydrogen-bonding of the OH and NH groups of acetaminophen are involved. These interactions can be disrupted by the perturbations induced by the surrounding CO_2 molecules on increasing the CO_2 concentration in the mixture in CO_2-expanded acetone in view of the dipole−dipole nature of the interactions between the CO groups of both acetaminophen and acetone. On this basis, it is possible to successfully interpret the solubility variation of acetaminophen with the CO_2 concentration in acetone and ethanol solvents.[1,2] Finally, we emphasize that the combination of the IR absorption spectrometry with a quantum chemistry approach is a valuable methodology to provide molecular insights about the preferential solvation mechanisms of acetaminophen in CO_2-expanded organic solvents.

Acknowledgment. The authors gratefully acknowledge the IDRIS computer centre of the CNRS (Institut du Développement et des Ressources en Informatique Scientifique, Orsay) and the MASTER of the ENSPCB (Université de Bordeaux I, Talence) for allocating computing time and providing facilities.

References and Notes

(1) Sala, S.; Danten, Y.; Ventosa, N.; Tassaing, T.; Besnard, M.; Veciana, J. *J. Supercrit. Fluids* **2005**, in press.
(2) Sala, S.; Tassaing, T.; Ventosa, N.; Danten, Y.; Besnard, M.; Veciana, J. *Chem. Phys. Chem.* **2004**, *5*, 243.
(3) Weber, A.; Yelash, L. V.; Kraska, T. *J. Supercrit. Fluids* **2005**, *33*, 107.
(4) Beckman, E. J. *J. Supercrit. Fluids* **2003**, *28*, 121.
(5) Shariati, A.; Petres, C. J. *J. Supercrit. Fluids* **2002**, *23*, 195.
(6) Brennecke, J. F. *Nature* **1997**, *389*, 333.
(7) Jung, J.; Perrut, M. *J. Supercrit. Fluids* **2001**, *20*, 179.
(8) Tom, J. W.; Debenedetti, P. G. *J. Aerosol Sci.* **1991**, 555.
(9) Gallagher, P. M.; Coffey, M. P.; Klasutis, V. J. *ACS Symp. Ser.* **1989**, *406*, 334.
(10) Matson, D. W.; Fulton, J. L.; Petersen, R. C.; Smith, R. D. *Ind. Eng. Chem. Res.* **1987**, *26*, 2298.
(11) Sala, S.; Ventosa, N.; Munto, M.; Veciana, J. Manuscript in preparation.
(12) Ventosa, N.; Sala, S.; Veciana, J. *J. Supercrit. Fluids* **2003**, *26*, 33.
(13) Ventosa, N.; Sala, S.; Torres, J.; Llibre, J.; Vecciana, J. *Cryst. Growth Des.* **2001**, *1*, 299.
(14) Frisch, M. J.; Trucks, G. W.; Schlegel, H. B.; P. M. W. Gill, B. G. J.; Robb, M. A.; Cheeseman, J. R.; Keith, T.; Peterson, G. A.; Montgomery, J. A.; Raghavachari, K.; Al-Laham, M. A.; Zakrewski, V. G.; J. V. Ortiz, J. B. F.; Ciolowski, J.; Stefanov, B. B.; Nanayakkara, A.; Challacombe, M.; Peng, C. U.; Ayala, P. Y.; Chen, W.; Wong, M. W.; Andres, J. L.; Replogle, E. S.; Comperts, R.; Martin, R. L.; Fox, D. J.; Binkley, J. S.; DeFrees, D. J.; Baker, J.; Steward, J. J. P.; Head-Gordon, M.; Gonzalez, C.; Pople, J. A. *Gaussian 99 Program*; 1998.
(15) Binev, I. G.; Vassileva-Boyadjieva, P.; Binev, Y. I. *J. Mol. Struct.* **1998**, *447*, 235.
(16) Perdew, J. P.; Burke, K.; Wang, Y. *Phys. Rev. B* **1996**, *54*, 16533.
(17) Perdew, J. P.; Chevary, J. A.; Vosko, S. H.; Jackson, K. A.; Pederson, M. R.; Singh, D. J.; Fiolhais, C. *Phys. Rev. B* **1992**, *46*, 6671.
(18) Perdew, J. P.; Chevary, J. A.; Vosko, S. H.; Jackson, K. A.; Pederson, M. R.; Singh, D. J.; Fiolhais, C. *Phys. Rev. B* **1993**, *48*, 11638.
(19) Scott, A. P.; Radom, L. *J. Phys. Chem.* **1996**, *100*, 16502.
(20) Rassolov, V. A.; Ratner, M. A.; Pople, J. A.; Redfern, P. C.; Curtiss, L. A. *J. Comput. Chem.* **2001**, *22*, 976.
(21) Rassolov, V. A.; Pople, J. A.; Ratner, M. A.; Windus, T. L. *J. Chem. Phys.* **1998**, *109*, 1223.
(22) Francl, M. M.; Pietro, W. J.; Hehre, W. J.; Binkley, J. S.; DeFrees, D. J.; Pople, J. A.; Gordon, M. S. *J. Chem. Phys.* **1982**, *77*, 3654.
(23) Blaudeau, J. P.; McGrath, M. P.; L. A. Curtiss; Radom, L. *J. Chem. Phys.* **1997**, *107*, 5016.
(24) BinningJr., R. C.; Curtiss, L. A. *J. Comput. Chem.* **1990**, *11*, 1206.
(25) McLean, A. D.; Chandler, G. S. *J. Chem. Phys.* **1980**, *72*, 5639.
(26) Krishnan, R.; Binkley, J. S.; Seeger, R.; Pople, J. A. *J. Chem. Phys.* **1980**, *72*, 650.
(27) Gordon, M. S. *Chem. Phys. Lett.* **1980**, *76*, 163.
(28) Hariharan, P. C.; Pople, J. A. *Mol. Phys.* **1974**, *27*, 209.
(29) Hehre, W. J.; Ditchfield, R.; Pople, J. A. *J. Chem. Phys.* **1972**, *56*, 2257.
(30) Ditchfield, R.; Hehre, W. J.; Pople, J. A. *J. Chem. Phys.* **1971**, *54*, 724.
(31) Boys, S. F.; Bernardi, F. *Mol. Phys* **1970**, *19*, 553.
(32) Mierzwicki, K.; Latajka, Z. *Chem. Phys. Lett.* **2003**, *380*, 654.
(33) Valiron, P.; Mayer, I. *Chem. Phys. Lett.* **1997**, *1997*, 46.
(34) Tury, L.; Dannenberg, J. J. *J. Phys. Chem.* **1993**, *97*, 2488.
(35) White, J. C.; Davidson, E. R. *J. Chem. Phys.* **1990**, *93*, 8029.
(36) Wilson, E. B.; Decius, J. C.; Cross, P. C. McGraw-Hill: New York, 1955.
(37) Sinha, P.; Boesch, S. E.; Gu, C.; Wheeler, R. A. *J. Phys. Chem. A* **2004**, *108*, 9213.
(38) Wong, M. W. *Chem. Phys. Lett.* **1996**, *256*, 391.
(39) Pople, J. A.; Scott, A. P.; Wong, M. W.; Radom, L. *Isr. J. Chem.* **1993**, *33*, 345.
(40) NIST, D. NIST Gas-Phase Infrared Database; WebBook de Chimie NIST (Version 69) ed.; NIST Standard Reference Data Program, 2005.
(41) Ganeshrinivas, E.; Sathyanarayana, D. N.; Machida, K.; Miwa, Y. *J. Mol. Struct. (THEOCHEM)* **1996**, *361*, 217.
(42) Danten, Y.; Tassaing, T.; Besnard, M. *J. Phys. Chem. A* **2005**, *109*, 3250.
(43) Sun, Y. P. In *Supercritical Fluid Technology in Material Science and Engineering*; M. Decker: New York, 2002.